

Abundances in the Neutral Interstellar Medium of I Zw 18 from *FUSE* Observations

A. Aloisi¹, S. Savaglio^{1,2}, T.M. Heckman¹, C.G. Hoopes¹, C. Leitherer³, & K.R. Sembach³

ABSTRACT

We report on new *FUSE* far-UV spectroscopy of the most metal-poor blue compact dwarf galaxy I Zw 18. The new data represent an improvement over previous *FUSE* spectra by a factor of 1.7 in the signal-to-noise. Together with a larger spectral coverage ($\lambda\lambda = 917\text{--}1188 \text{ \AA}$), this allows us to characterize absorption lines in the interstellar medium with unprecedented accuracy. The kinematics averaged over the large sampled region shows no clear evidence of gas inflows or outflows. The H I absorption is interstellar with a column density of $2.2_{-0.5}^{+0.6} \times 10^{21} \text{ cm}^{-2}$. A conservative 3σ upper limit of $5.25 \times 10^{14} \text{ cm}^{-2}$ is derived for the column density of diffuse H₂. From a simultaneous fitting of metal absorption lines in the interstellar medium, we infer the following abundances: $[\text{Fe}/\text{H}] = -1.76 \pm 0.12$, $[\text{O}/\text{H}] = -2.06 \pm 0.28$, $[\text{Si}/\text{H}] = -2.09 \pm 0.12$, $[\text{Ar}/\text{H}] = -2.27 \pm 0.13$, and $[\text{N}/\text{H}] = -2.88 \pm 0.11$. This is in general several times lower than in the H II regions. The only exception is iron, whose abundance is the same. The abundance pattern of the interstellar medium suggests ancient star-formation activity with an age of at least a Gyr that enriched the H I phase. Around 470 SNe Ia are required to produce the iron content. A more recent episode that started 10 to several 100 Myr ago is responsible for the additional enrichment of α -elements and nitrogen in the H II regions.

Subject headings: galaxies: dwarf — galaxies: starburst — galaxies: individual (I Zw 18) — galaxies: ISM — ISM: abundances

¹Department of Physics & Astronomy, Johns Hopkins University, Baltimore, MD 21218

²On leave of absence from INAF-Osservatorio Astronomico di Roma, Italy

³Space Telescope Science Institute, Baltimore, MD 21218

1. Introduction

Within the well-accepted framework of hierarchical galaxy formation, dwarf ($M \lesssim 10^9 M_\odot$) galaxies are the first systems to collapse and start forming stars in the early Universe, supplying the building blocks from which more massive galaxies form later through merging and accretion (White & Rees 1978; Dekel & Silk 1986; Ikeuchi & Norman 1987). Many dwarfs, however, survive and end up intact in the local Universe, where they still represent the most common kind of galaxy observed at the present time (Marzke & da Costa 1997).

As remnants of the galaxy-formation process, present-day dwarfs may have been sites of the earliest star formation activity in the Universe. However, this hypothesis is challenged by the physical properties of blue compact dwarf (BCD) galaxies. BCDs have very blue colors typical of young stellar systems. They are currently experiencing intense star-formation (rates of $0.01\text{--}10 M_\odot \text{ yr}^{-1}$; Thuan 1991), but still contain large H I reservoirs (a few times $10^8 M_\odot$; Thuan & Martin 1981). Their properties are consistent with relatively short duration (\ll a Hubble time) for the ongoing burst. They are also characterized by low metal abundances (between about $Z_\odot/2$ and $Z_\odot/50$ as inferred by H II region observations; Thuan et al. 1994), indicative of a chemically unevolved interstellar medium (ISM), and some of them contain much less heavy-element enrichment than the majority of the observed high-redshift galaxies. The most metal-poor ($Z \lesssim 1/20 Z_\odot$) BCDs have been pointed out as good candidate “primeval” galaxies in the nearby Universe, with ages less than 100 Myr as inferred from their chemical properties (Izotov & Thuan 1999). If indeed some BCDs turn out to be young galaxies, their existence would support the view that star formation in low-mass systems has been inhibited till the present epoch (e.g., Babul & Rees 1992). Unveiling the evolution of extreme BCDs is thus of primary importance for understanding galaxy formation and evolution.

The evolution of a galaxy is driven by the evolution of its primary constituents, stars and gas. Stars have a key role in consuming and returning gas, producing luminous and mechanical energy, and synthesizing nearly all elements heavier than He in the Universe. Stars chemically influence the surrounding ISM depending on their mass: α -elements (e.g., O) are mostly released by SNe II from massive stars on short time scales ($\lesssim 50$ Myr); C and N are mainly produced by intermediate-mass stars on longer time scales ($\gtrsim 300$ Myr); Fe is principally supplied by SNe Ia on time scales $\gtrsim 1$ Gyr. This can lead to unusual non-solar abundance ratios of the ISM when coupled with the extreme star-formation histories of BCDs. A high level of star formation can pollute the gas with α -elements and result in an overall α/Fe enhancement. On the other hand, the contribution from SNe Ia during a long quiescent period can significantly increase the Fe content, thus considerably decreasing the α/Fe ratio. The situation can also be complicated by the presence of strong galactic

winds triggered by SNe II that, coupled with the shallow gravitational potential of low-mass systems, can differentially eject metals into the intergalactic medium (e.g. De Young & Heckman 1994; Marlowe et al. 1995).

The chemical properties of the ISM are, therefore, a fossil record of the star-formation history of a galaxy. However, different spectroscopic abundance estimators sample different elements, as well as different phases of the ISM and different look-back times. Measured abundances in the gaseous component also depend on how well, and on what time scale, the ISM is mixed, and on what time scale freshly produced metals cool and become visible. The chemical homogeneity of the H II regions (e.g., Kobulnicky & Skillman 1996, 1997) suggests that mixing is quick and efficient in dwarf systems. Emission lines from warm ($T \simeq 10^4$ K) ionized gas have long been the primary chemical diagnostic in the ISM of star-forming galaxies. This technique is highly refined and well constraining, especially in the determination of O abundances (e.g., Skillman 1998). H II regions probe the state of the gas at the birth of massive stars (a few Myr ago). However, they may already be self-polluted with very recently produced metals (Kunth & Sargent 1986). X-ray observations offer abundance indicators for the hot ($T \simeq 10^6 - 10^8$ K) phase of the ISM (Persic et al. 1998; Martin, Kobulnicky, & Heckman 2002), probing the metals released during the ongoing burst that are still trapped within the galactic wind and are not yet mixed with the photoionized gas. UV absorption lines from neutral gas supply another way to infer the metallicity of the ISM. These lines sample lower temperature regions ($T \lesssim 10^4$ K) which are less likely to be involved in the star-formation, thus avoiding more the problem of self-pollution.

Metal abundances of BCDs have been widely investigated in the past through detailed studies of H II regions (e.g., Izotov & Thuan 1999). However, chemical properties of other ISM phases still remain missing pieces of a complicated puzzle. The H I content in BCDs is only $\sim 10\%$ of the dynamical mass (which is dominated by dark matter), but amounts to $\sim 90\% - 95\%$ of the total baryonic mass (e.g., Kniazev et al. 2000). As the dominant component of the baryonic matter, neutral gas could hide the bulk of metals. Of necessity, we must correctly address this issue in order to understand the chemical (and physical) evolution of BCDs. Recently, the launch of the *Far Ultraviolet Spectroscopic Explorer* (*FUSE*; Moos et al. 2000) has provided access to the rich system of far-UV absorption lines. The strong blue continua of the spectra, combined with the high sensitivity and resolution of *FUSE* in the 900–1200 Å wavelength range, allow us for the first time a characterization of the metal content in the neutral ISM of BCDs. Prior to *FUSE*, a similar analysis of the rest-frame UV spectra has been possible only for the high-redshift absorbing systems along the lines of sight to quasars (e.g., Lu et al. 1996) or for the gravitationally lensed Lyman break galaxy MS 1512–cB58 at $z = 2.7276$ (Pettini et al. 2002), thanks to the superior sensitivity of telescopes and spectrographs in the optical. Up to now only *FUSE* spectra of the BCDs

I Zw 18 (Vidal-Madjar et al. 2000; Levshakov, Kegel, & Agafonova 2001), Mrk 59 (Thuan, Lecavelier des Etangs, & Izotov 2002), and NGC 1705 (Heckman et al. 2001) have already been published. However, I Zw 18 has been re-observed by *FUSE* with an additional $\sim 60,000$ s of integration time (only $\sim 30,000$ s are available for the first dataset) since the publication of the data. I Zw 18 is also one of the most interesting and modelled BCDs in the local Universe. For all these reasons, we have retrieved from the archive, combined, and analyzed the two *FUSE* datasets of I Zw 18. This paper reports the results of our analysis.

Discovered by Zwicky in 1966, I Zw 18 remains the BCD with the lowest metallicity inferred from the oxygen content of its H II regions ($1/50 Z_{\odot}$; e.g., Izotov & Thuan 1999). Although it is often referred to as “the most metal-poor galaxy known”, it is still two orders of magnitude more metal rich than the most metal-poor stars in the Milky Way ($\text{Fe}/\text{H} \simeq -4$; Cayrel 1996). I Zw 18 has always been regarded as the best candidate for a truly “young” galaxy in the local Universe, with an estimated age less than 40 Myr (Izotov & Thuan 1999). Its youth has, however, been questioned by the recent HST discovery in the optical (Aloisi, Tosi, & Greggio 1999) and near-infrared (Östlin 2000) of a well-defined population of asymptotic giant branch (AGB) stars at least several hundred Myr and possibly up to a few Gyr old. Moreover, detailed modeling of broad-band colors in the optical and near infrared (Hunt, Thuan, & Izotov 2003) has shown that ages of a few hundred Myr are in better agreement with the integrated properties of I Zw 18, even if as much as 22% of the total mass could be contributed by older stars. Due to its very peculiar nature, I Zw 18 has been extensively studied for the last three decades, but its evolutionary state still remains a matter of debate.

The distribution and kinematics of I Zw 18 neutral hydrogen from aperture-synthesis observations have been discussed by several authors. The dynamical and H I masses are $\lesssim 10^9 M_{\odot}$ and $\lesssim 10^8 M_{\odot}$, respectively (Lequeux & Viallefond 1980; Viallefond, Lequeux, & Comte 1987; van Zee et al. 1998b). Van Zee et al. (1998b) have revealed a complex H I morphology with a neutral gas velocity dispersion of $\sigma \simeq 12\text{--}14 \text{ km s}^{-1}$. Martin (1996) and Petrosian et al. (1997) have discussed the complicated velocity field of the ionized component. The H I column density has been estimated to be as high as $N(\text{HI}) \simeq 2\text{--}3 \times 10^{21} \text{ cm}^{-2}$ (Kunth et al. 1994; Vidal-Madjar et al. 2000). More recently, from their *STIS* data at $0''.5$ spatial resolution Brown et al. (2002) have discovered significant inhomogeneity in the neutral gas of I Zw 18 with a peak ~ 10 times higher than previously estimated. Molecular gas has not been detected in I Zw 18, either through CO emission in the mm (Gondhalekar et al. 1998) or through H₂ absorption in the far-UV (Vidal-Madjar et al. 2000). Low extinction is reported in most studies, and the galaxy has not been detected by the Infra-Red Astronomical Satellite (*IRAS*). This could be an indication of a low and/or clumpy dust content in I Zw 18 (Cannon et al. 2002), consistent with the low metallicity and *FUSE* non-detection of diffuse

H₂ (Vidal-Madjar et al. 2000).

Abundances derived from H II regions are reasonably well known in I Zw 18 (Searle & Sargent 1972; Dufour, Garnett, & Shield 1988; Skillman & Kennicutt 1993; Garnett et al. 1995a, 1995b; Garnett et al. 1997; Izotov & Thuan 1999; Izotov et al. 1999). These studies indicate a low O content, but rather high N/O and C/O ratios (suggestive of an intermediate-age stellar population; e.g., Dufour et al. 1988), as well as a high degree of uniformity in the nebular abundances. The metal content in the H I component of I Zw 18 is instead more uncertain. Kunth et al. (1994) have attempted a first measurement of O in the neutral gas phase, and found a metallicity 20 times lower than in the H II regions. Pettini & Lipman (1995) have, however, shown that the observations of Kunth et al. cannot constrain the metallicity of the neutral gas due to saturation of the UV absorption line used, O I λ 1302. Combining the analysis of Pettini & Lipman (1995) with their new value for the H I dispersion, van Zee et al. (1998b) have instead derived an H I metallicity more similar to that in the H II regions. Also Levshakov et al. (2001) have recently suggested a good degree of mixing between warm and cold gaseous phases. At the opposite extreme, Izotov, Schaerer, & Charbonnel (2001) have claimed primordial abundances for the neutral gas in I Zw 18 by investigating the possibility that UV absorption lines arise from H II regions.

Our new *FUSE* observations will certainly help to address many of the abundance issues in I Zw 18. These data represent an improvement over *FUSE* spectra previously published by Vidal-Madjar et al. (2000) and used for metal abundance determinations by Levshakov et al. (2001). The signal-to-noise ratio (S/N) is higher by a factor of 1.7, and the covered spectral range is wider ($\lambda\lambda = 917\text{--}1188 \text{ \AA}$ versus $\lambda\lambda = 979\text{--}1188 \text{ \AA}$). We are able to estimate abundances of O, Si, Ar, Fe and N in the neutral gas of I Zw 18 with unprecedented accuracy, thanks to the availability of several lines per ion and the application of a procedure allowing for their simultaneous fit. We find that the metal content in the neutral gas is significantly lower than in the H II regions, apart from Fe, which is the same. A certain amount of ancient star-formation is required to reproduce the observed abundance patterns. The paper is outlined as follows. We describe the *FUSE* observations and data reduction in section 2. The analysis of *FUSE* data and its caveats are presented in section 3. The problem of the systemic velocity is addressed in section 4. Section 5 presents an estimate of the H I column density. We derive a 3σ upper limit on the amount of diffuse H₂ in section 6. Heavy element abundances of the neutral ISM are derived in section 7. Section 8 presents our findings in the context of the chemical evolutionary state of I Zw 18. The summary and conclusions are given in section 9.

2. *FUSE* Observations and Data Reduction

Two *FUSE* datasets for I Zw 18 ($\alpha_{2000} = 09^h 34^m 01^s.92$, $\delta_{2000} = +55^\circ 14' 26''.1$; $l_{II} = 160^\circ 52' 61.0$, $b_{II} = +44^\circ 84' 18.3$) were obtained on 1999 November 27 and 2001 February 11, respectively, as part of *FUSE* Team programs P198 and P108. The first observations detected the target only in the LiF channels ($\lambda\lambda = 979\text{--}1188 \text{ \AA}$) for a total exposure time of $\sim 31,600$ s, $\sim 30\%$ of which occurred during the orbital night. These spectra have been extensively analyzed by Vidal-Madjar et al. (2000) and Levshakov et al. (2001). The most recent dataset includes both LiF and SiC channels ($\lambda\lambda = 905\text{--}1188 \text{ \AA}$) for a total integration time of $\sim 63,500$ s, of which $\sim 60\%$ occurred during orbital night. In both observing runs I Zw 18 was centered in the large aperture (LWRS, $30'' \times 30''$) which amply covered the whole galaxy.

The data were retrieved from the MAST archive and processed with the latest release of the *FUSE* calibration pipeline (version 2.0). This was, however, updated to include the new set of background files and the correct error estimate that were later available in version 2.1⁴. The first part of the pipeline was applied to individual exposures in order to get correct Doppler shifts and grating motions from the orbital parameters in the headers of single images. All exposures relative to each dataset were then combined with the CALFUSE task “ttag_combine”, taking into account residual velocity offsets. We finally ran the last part of the calibration pipeline on the final combined raw images. This non-standard procedure allowed for a better estimate of the background and a more accurate spectral extraction in case of faint sources. A binning by a factor of 6 was applied to the data in order to improve the identification of spectral features without degrading the spectral resolution. The extracted 1D spectra, one per dataset, were then combined together to obtain a unique spectrum with an exposure time around 95,100 s and 63,500 s in the LiF and SiC channels, respectively. This increased the S/N per resolution element by a factor of ~ 1.7 in the LiF channels compared to the original spectra, and extended the spectral coverage to $\lambda < 979 \text{ \AA}$ in the SiC channels. Residual wavelength shifts among different segments were then estimated and applied using the LiF 1A channel as a reference. A remaining zero-point wavelength offset of $\lesssim 0.10 \text{ \AA}$ was corrected by requiring the Galactic ISM lines to fall at $\sim 0 \text{ km s}^{-1}$.

We avoided combining data from the eight different channels into one composite spectrum over the whole *FUSE* spectral range because the instrumental resolution and sensitiv-

⁴It has been later discovered (FUSE User’s Electronic Newsletter no. 25 of 2003 March 17) that the calculation of the errors in the FUSE calibration pipeline version 2.1 has a bug that could underestimate the real value of the errors for bright sources. This clearly does not affect faint targets like I Zw 18.

ity vary as a function of wavelength. We instead constructed a final spectrum in the interval $\lambda\lambda = 917\text{--}1188 \text{ \AA}$ by adding together segments of spectra taken from the channel with the highest sensitivity in a certain wavelength region, mainly SiC 2A, LiF 1A, and LiF 2A. The redundant information at lower S/N contained in the segments not used was, however, considered for a consistency check.

Only data taken during the orbital night (with a S/N lower by a factor of 1.3) were considered in those parts heavily contaminated by emission from terrestrial O I and N I airglow. This procedure was applied in order to minimize geocoronal contamination. We expected emission from geocoronal lines to be practically absent in the so-called “night” data. This can be easily verified by an eye inspection of the final spectrum, where, e.g., the saturated O I $\lambda 1039$ absorption from the Milky Way goes to zero intensity, indicating practically no residual contribution from one of the strongest airglow lines. On the other hand, absorption lines in I Zw 18 are redshifted of a few pixels (e.g., $\sim 2.5 \text{ \AA}$ for O I $\lambda 1039$), so that residual airglow contamination does not represent a problem in any case.

A nominal spectral resolution of $\Delta\lambda/\lambda \simeq 10000$, corresponding to $v \simeq 30 \text{ km s}^{-1}$, was derived by taking into account the aperture and the size of the galaxy ($10''$). An observed upper limit around 40 km s^{-1} was instead estimated by measuring the FWHM of the narrowest H₂ lines arising from the Milky Way (MW). A final spectral resolution of $35 \pm 5 \text{ km s}^{-1}$ over the whole wavelength range was finally adopted. The noise spectrum was calculated through photon statistics propagation of object and sky spectra. The final S/N is $\sim 7, 17, \text{ and } 18$ per resolution element at 950 \AA (SiC 2A), 1050 \AA (LiF 1A), and 1150 \AA (LiF 2A).

The fit of the continuum was performed by interpolating between points of the observed flux free of apparent absorption. This is not particularly easy because of the limited S/N of the spectrum. Members of the team independently estimated the continuum for a consistency check, and the differences were always well below the noise uncertainties. Errors associated with measured quantities in the *FUSE* spectrum are from counting statistics only and were calculated from the S/N of the data. Systematic errors due to the uncertainty in the continuum placement were not considered.

The resulting final *FUSE* spectrum of I Zw 18 is shown in Fig. 1. Three absorption line systems at three different radial velocities are clearly present: the well-known high-velocity cloud (HVC) at -160 km s^{-1} , the Milky Way (MW) at 0 km s^{-1} , and I Zw 18 at $\sim 750 \text{ km s}^{-1}$. The high-velocity cloud and Galaxy systems have already been briefly discussed by Vidal-Madjar et al. (2000), and will not be detailed further. Here we will concentrate on the absorption line system in I Zw 18.

3. Analysis of *FUSE* Data and Caveats

We derived column densities of H I and heavy elements from the *FUSE* spectra of I Zw 18 by line-profile fitting of the observed absorption lines. Standard theoretical Voigt profiles were convolved with the gaussian instrumental resolution and fitted to the data. The package FITLYMAN (Fontana & Ballester 1995) in MIDAS for multi-component fitting was used for this purpose. This method is more powerful than a simple curve-of-growth analysis (based on the equivalent width of the absorption lines) because it allows for *i*) the deblending of multiple components along the line of sight contributing to the same absorption, and *ii*) the simultaneous and independent fit of contaminating absorption components. We were able to fit absorption lines of all the ions considered in I Zw 18 with very simple velocity component models (one component, except for Fe II where two components were necessary).

The real physical situation described by I Zw 18 far-UV spectra is, however, more complex. *FUSE* detects a non-linear average absorption over the full extent of the stellar background sources, since its large aperture includes the whole galaxy. This implies that the observed lines arise from a combination of many unresolved velocity components from different absorbing clouds along the many lines of sight. Moreover, some lines of sight may have saturated absorption, even if the composite profile does not go to zero intensity (e.g., Savage & Sembach 1991).

Jenkins (1986), on the other hand, has demonstrated that the single-velocity approximation (one-velocity component) applied to complex blends of features gives nearly the correct answer (the simulated-to-true column density ratio rarely goes below 0.8) if the distribution function for the line characteristics is not irregular (e.g., bimodal, see also Savage & Sembach 1991). This result holds also if different lines have different saturation levels or Doppler parameters b . Since our *FUSE* data of I Zw 18 average over the whole galaxy, we expect a quite regular distribution of the kinematical properties of the single absorbing components. We thus believe we amply fall within the regime where the single-velocity approximation is valid.

In light of these considerations, we preferred to maintain a simple approach in the determination of the column densities with the line-profile fitting method. We thus avoided the introduction of additional free parameters, i.e. the number of intervening clouds and their velocity distribution, since we believe the resolution of the data does not allow to correctly constrain the real physical situation represented by this type of observation. In the single-velocity approximation the fitting parameter b has no precise physical meaning, but is rather the result of the combination of both the various line Doppler widths present (due, e.g., to turbulent and/or thermal broadening) and the various velocity separations among the different line components (Hobbs 1974). On the other hand, according to Jenkins (1986)

the column density is well constrained. In addition, the column density of a certain ion is even better constrained if several lines with different values of $f\lambda$ (λ is the rest-frame wavelength and f the oscillator strength of the absorption) are available for a simultaneous fit, and the results are independent of saturation problems affecting the strongest lines.

However, in order to check the quality of the results with the line-profile fitting and the single-velocity approximation, we also determined total column densities of heavy elements by applying the apparent optical depth method (Savage & Sembach 1991). The apparent column density of an ion in each velocity bin, $N_a(v)$ in units of $\text{cm}^{-2} (\text{km s}^{-1})^{-1}$, is related to the apparent optical depth in that bin $\tau_a(v)$ by the expression:

$$N_a(v) = \frac{m_e c}{\pi e^2} \frac{\tau_a(v)}{f\lambda} = 3.768 \times 10^{14} \frac{\tau_a(v)}{f\lambda(\text{\AA})}. \quad (1)$$

The apparent optical depth is directly calculated from the observed intensity in the line at velocity v , $I_{\text{obs}}(v)$, by

$$\tau_a(v) = -\ln [I_{\text{obs}}(v)/I_0(v)], \quad (2)$$

where $I_0(v)$ is the intensity in the continuum. $N_a(v)$ is an apparent column density per unit velocity because its value depends on the resolution of the spectrograph and on the apparent shape of the line. The total apparent column density, N_a , is obtained by direct integration of equation (1) over the velocity interval where line absorption takes place

$$N_a = \int N_a(v) dv. \quad (3)$$

In the limit where the absorption line is weak ($\tau \ll 1$) or fully resolved (the FWHM of the line is larger than the instrumental FWHM), the total apparent column density N_a and the true column density N are equal.

The apparent optical depth method is very powerful for determining column densities. Its strength lies in the fact that no assumption needs to be made concerning the velocity distribution of absorbers, i.e., it does not depend on the number of intervening clouds along the single or multiple lines of sight. However, it does not provide a correct answer for quite strong lines that are not fully resolved. In the case of our resolution of $\sim 35 \text{ km s}^{-1}$, the line-profile fitting should give a more accurate measure of the ionic column densities compared to the apparent optical depth method, especially for stronger lines. The latter can nevertheless be more potent in unveiling hidden saturation if two or more lines with relatively different $f\lambda$ values are available. Such a situation will easily manifest itself with a column density from the apparent optical depth method being smaller for lines with higher $f\lambda$ values. In our analysis, the similarities between the column densities obtained with the line-profile fitting and the apparent optical depth method for weak (and thus, more optically thin)

lines ($W_0 \lesssim 200 \text{ m\AA}$) strengthen our results, and justify the single-velocity approximation approach (§ 7.1).

Finally, we want to point out another caveat generic to this type of *FUSE* observations where the whole star-forming galaxy is included in the spectroscopic aperture. The far-UV radiation we detect is the one not intercepting the opaque dense clumps with a high dust and molecular content (even if with a very low covering factor; Hoopes et al. 2003b). The far-UV light is thus biased toward lower metallicity regions. The more diffuse ISM, however, can contain a certain amount of dust (Meurer, Heckman, & Calzetti 1999; Hoopes et al. 2003b), thus of metals. In addition, there are indications from UV/optical studies that the dust content in I Zw 18 is relatively low (Meurer et al. 1999; Cannon et al. 2002). We hence do not expect that our results are heavily biased toward regions with lower metallicity. Nevertheless, the strongest result of our analysis, i.e. the metal enrichment of the neutral gas, would still remain valid even in case dust plays an important role.

4. The Systemic Velocity of I Zw 18

The *FUSE* spectrum of I Zw 18 exhibits a multitude of stellar and interstellar lines. Most of the stellar lines are blends of multiple transitions. The strongest and cleanest photospheric line is C III $\lambda 1176$, although this is a multiplet centered at 1175.6 \AA . We observed this line at a central wavelength of $\lambda = 1178.59 \pm 0.04 \text{ \AA}$, taking into account that its red side could be contaminated by a P-Cygni profile from stellar winds of OB supergiants. We inferred a redshift of $z_{\text{stars}} = 0.00254 \pm 0.00003$, corresponding to a systemic velocity of $v_{\text{stars}} = 761 \pm 9 \text{ km s}^{-1}$. Exactly the same result is independently obtained for the other strong C III line at 977 \AA , whose nature is more uncertain since it can arise from both the photosphere and the interstellar medium. Our value of v_{stars} is very similar to the mean value of $v_{\text{HII}} \simeq 763 \text{ km s}^{-1}$, obtained by Petrosian et al. (1997) from an $\text{H}\alpha$ interferometric study of both the northwest and southeast H II regions ($v_{\text{HII}} = 742 \pm 7 \text{ km s}^{-1}$ and $783 \pm 5 \text{ km s}^{-1}$, respectively). Within the errors, v_{stars} is also consistent with $v_{\text{HI}} = 751 \pm 2 \text{ km s}^{-1}$ derived by Thuan et al. (1999) for the H I component. Here we will adopt $z_{\text{stars}} = 0.00254$ as the redshift of I Zw 18 and $v_{\text{stars}} = 761 \text{ km s}^{-1}$ as its systemic velocity.

5. H I Column Density

The good S/N and high resolution of the *FUSE* spectrum of I Zw 18 give us, in principle, a unique opportunity to study the absorption lines of the H I Lyman series from Ly β to Ly μ

(H I 12). In practice only the absorptions up to Ly η (H I 7) were used, because the higher order lines were completely contaminated by Galactic H₂ and other interstellar lines. Ly α at $\lambda = 1215.67 \text{ \AA}$ is outside the covered spectral range (Fig. 1). The foreground H I column density in the direction of I Zw 18 due to the Milky Way is $\sim 2 \times 10^{20} \text{ cm}^{-2}$ (Stark et al. 1992), while the high-velocity cloud contribution is $\sim 2.1 \times 10^{19} \text{ cm}^{-2}$ (Kunth et al. 1994).

The H I absorption lines of I Zw 18 appear to be narrow, and thus interstellar in origin. However, *FUSE* spectra of Galactic early B stars (Pellerin et al. 2002) clearly show the presence of a broad photospheric component (e.g., their Fig. 3). This implies that when early B stars start to dominate the integrated spectrum of a stellar population (e.g., a burst with an age greater than ~ 10 Myr), the wings of a large photospheric contribution are superposed on the cores of the narrow interstellar absorption. The same conclusion is reached by González-Delgado, Leitherer, & Heckman (1997) through their comparison of observed and synthetic profiles of O VI $\lambda\lambda 1032, 1038 + \text{Ly } \beta + \text{C II } \lambda\lambda 1036, 1037$ (see their Fig. 4).

The age of the stellar population dominating the emission-line UV/optical spectra of I Zw 18 is quite well defined. De Mello et al. (1998) have derived spectral information on the northwest star-forming region from the literature, and dated its stellar content with stellar evolutionary synthesis models at a metallicity of $Z = 0.0004$. They have suggested an instantaneous burst with an age around 3 Myr, as indicated by the observed Wolf-Rayet stellar features and the equivalent width of H β . On the other hand, Mas-Hesse & Kunth (1999) have inferred the age of I Zw 18 from ground-based optical spectroscopy of the whole galaxy. The evolutionary synthesis models they have applied present a degeneracy for the best solution: a continuous star formation with an age of 13 Myr (this model is preferred by these authors), and a 3 Myr old instantaneous burst. Mas-Hesse & Kunth have also been able to assess that the underlying older stellar component, (as indicated by studies on I Zw 18 resolved stellar population), would not affect the dating of the observed spectrum.

At present it is not possible to determine the age of I Zw 18 stellar population by applying stellar evolutionary synthesis codes to the *FUSE* data. We have recently implemented a *FUSE* stellar library of stars from the Milky Way and Magellanic Clouds into Starburst99 (Robert et al. 2003). This implies that the synthesis of stellar populations in the spectral range $\sim 1003\text{--}1188 \text{ \AA}$ is available, but still limited to solar and 1/5 solar metallicities. We are investigating the possibility of implementing Starburst99 with a stellar library of theoretical stellar atmosphere spectra at extremely low metallicities (Kudritzki 2002). This will allow us to correctly date I Zw 18 stars in the far-UV band in the near future. In this paper we will assume that the *FUSE* spectrum is dominated by hot O stars from star-forming regions (as previously suggested by other authors). The additional presence of B or

later-type stars would not affect an O-dominated far-UV spectrum due to the much lower luminosities contributed by these stars; e.g., a late-type O star with $T \simeq 30,000$ K at 1100 \AA has a luminosity which is ~ 100 times higher than that of a middle-type B star with $T \simeq 15,000$ K, and this difference is even larger if later-type stars are considered (Kurucz 1979). We thus expect that the wings of H I lines are not contaminated by broad photospheric absorption in I Zw 18. A single narrow interstellar component has been also considered by Vidal-Madjar et al. (2000) for the determination of H I column density from their *FUSE* spectra of I Zw 18. Moreover, in their analysis of *FUSE* data of Mrk 59, Thuan et al. (2002) explicitly mention contamination of H I Lyman series lines by broad photospheric absorption. They attribute the difference in photospheric contamination between I Zw 18 and Mrk 59 to the older age of the latter.

We reproduced the shape of the H I Lyman series lines in I Zw 18 through profiles characterized by a single component with a column density of $N(\text{HI}) = 2.2_{-0.5}^{+0.6} \times 10^{21} \text{ cm}^{-2}$. Fig. 2 shows the Lyman series lines with the best theoretical model. Only the red wing of $\text{Ly}\beta$ was used to constrain the model parameters, since the blue wing is contaminated by $\text{Ly}\beta$ absorption from the Galaxy and the high-velocity cloud, as well as by geocoronal emission. Due to its damped profile, $\text{Ly}\beta$ is a very strong constraint to the H I column density. This is valid also in our case, where the Lyman series lines of higher order show some contamination by interstellar absorptions, except for $\text{L}\eta$. On the other hand, $\text{L}\eta$ is saturated but not damped, thus its profile is much more sensitive to the Doppler parameter.

Our H I column density is perfectly consistent with the value of $2.1 \times 10^{21} \text{ cm}^{-2}$ that Vidal-Madjar et al. (2000) obtained from $\text{Ly}\beta$ absorption in their *FUSE* spectrum. It is also similar to, but slightly less than, the value of $3.5 (\pm 0.5) \times 10^{21} \text{ cm}^{-2}$ inferred by Kunth et al. (1994) from $\text{Ly}\alpha$ absorption. In addition, the systemic velocity of $v_{\text{HI}} = 753 \pm 6 \text{ km s}^{-1}$ ($z_{\text{HI}} = 0.00251 \pm 0.00002$) we inferred for the H I gaseous component, is compatible with the value derived by Thuan et al. (1999) from 21-cm observations ($v_{\text{HI}} = 751 \pm 2 \text{ km s}^{-1}$).

Brown et al. (2002) have recently obtained *STIS* data of I Zw 18 at $0''.5$ spatial resolution and inferred the H I column density from $\text{Ly}\alpha$ absorption at different locations within the galaxy. They have discovered significant inhomogeneity in the neutral gas, with a peak as high as $N(\text{HI}) \simeq 2 \times 10^{22} \text{ cm}^{-2}$ in the fainter (southeast) part of the galaxy, and a density quickly dropping to a value 10 times lower as soon as a slightly different line of sight is considered. Our *FUSE* estimate of $N(\text{HI})$ is ~ 10 times lower than the peak value measured by Brown et al., but the difference can be easily ascribed to the different nature of the observations. *FUSE* data have been acquired through an aperture much larger than the whole extension of I Zw 18. *STIS* data are instead a collection of 7 different long-slit observations covering a large fraction of the galaxy, but not its totality. As a consequence,

our data are clearly a non-linear average value of the H I column density over many lines of sight through the galaxy, and are probably consistent with the Brown et al. results, once smearing of the higher spatial resolution information is correctly taken into account.

The Doppler parameter for the best theoretical model of the H I absorption lines is $b = 35 \pm 10 \text{ km s}^{-1}$. Taking into account that *FUSE* data are sampling an average absorption (§ 3), this value of b does not have a real physical meaning, being associated with unresolved multiple velocity components along the various lines of sight. For comparison, the instrumental broadening due to our spectral resolution is around 21 km s^{-1} , too low to resolve the various velocity components with typical temperatures $T \lesssim 10^4 \text{ K}$ if they are dominated by thermal broadening (in this case $b \lesssim 10 \text{ km s}^{-1}$). On the other hand, the velocity dispersion of $\sigma \simeq 12\text{--}14 \text{ km s}^{-1}$, as inferred from radio observations (van Zee et al. 1998b), would lead to a value of $\sim 20 \text{ km s}^{-1}$ ($b = \sqrt{2}\sigma$) for single velocity components where broadening is dominated by turbulent motions. It is interesting to notice that there is a velocity gradient of about 50 km s^{-1} in the H I component across the area covered by the *FUSE* beam (van Zee et al. 1998b). It could be that most of our large Doppler parameter is due to this gradient, since the far-UV light from the background stars probably samples a large fraction of this range in H I velocity.

6. Upper Limits on the Diffuse H₂ Content

H₂ absorption lines from the Milky Way are clearly visible in the I Zw 18 spectrum (Fig. 1). However, no lines of H₂ are seen at the radial velocity of the BCD, despite the fact that I Zw 18 has a total H I column density higher than that measured on average in the Milky Way. Vidal-Madjar et al. (2000) estimated a 10σ upper limit of 10^{15} cm^{-2} for the molecular hydrogen column density. In this paper we re-addressed this issue by taking advantage of the higher S/N *FUSE* spectrum.

We inferred an upper limit to the H₂ column density of I Zw 18 with the following procedure. For each of the first five ($J = 0\text{--}4$) rotational levels of H₂ intrinsic to I Zw 18 we selected the strongest unblended line providing the most stringent constraint to the inferred column density in each level, we measured the noise at its predicted location and we calculated an upper limit to its rest-frame equivalent width W_0 . The transitions considered for this purpose are indicated in Table 1 together with their W_0 values. Since we were dealing with upper limits for the equivalent width, we could not apply the curve-of-growth technique and estimate a total H₂ column density. Therefore, we converted the W_0 upper limits of each transition into column density upper limits by assuming the optically thin case, corresponding to the linear part of the curve of growth (Spitzer 1978). The derived

values of N_J are listed in Table 1.

The absorption lines of the $J \geq 2$ levels are intrinsically weaker than those of the $J = 0$ and $J = 1$ levels, resulting in less restrictive upper limits on the column densities of those levels. Since the bulk of the column density is contained in the lower levels, deriving a limit on total H_2 by simply summing the upper limits for all the levels will be weighted toward the higher J levels and thus will produce an unrealistically high upper limit. We can improve the constraints on total H_2 if we take into account the likely distribution of the level populations.

Level populations for H_2 are typically described by a two-temperature Boltzmann distribution (see, e.g., Sembach et al. 2001). The kinetic temperature is usually suitable to describe the situation for $J = 0$ and $J = 1$ levels, since the densities are high enough that collisions determine the level populations. The populations of higher levels can be affected by other processes, like UV photon pumping, shocks, and formation of H_2 on dust grains (see Shull & Beckwith 1982 and references therein), and are usually better described by a higher excitation temperature. In both cases, the temperatures are derived from the ratios of column densities N_J and statistical weights g_J following Spitzer, Cochran, & Hirshfeld (1974).

Our procedure for setting an upper limit on total H_2 column density is as follows. For the $J = 0$ and $J = 1$ levels we simply add the two measured upper limits. For the higher J levels we assume a temperature, which establishes the level populations, and then normalize the level populations so that they do not violate any of the measured upper limits. Figure 3 shows how this is done in an excitation diagram. The 3σ upper limit to the column density N_J of each J level, divided by its statistical weight g_J , is plotted against excitation energy E_J . One of the two dashed lines in Fig. 3 shows the prediction for the extreme case of an excitation temperature of $T = 1000$ K. While this temperature is quite high for interstellar H_2 , comparable temperatures have been observed in supernova remnants (e.g., Welsh, Rachford, & Tumlinson 2002), so it may be applicable to starburst regions. Lower temperatures would give lower total column densities, so adopting 1000 K gives a conservative upper limit. The level populations are normalized so that they do not violate any of the observed upper limits, which means the total column density for the higher levels is dictated by the $J = 1$ upper limit. Note that this assumed temperature is used only to estimate the level populations, and that we cannot measure the excitation temperature in the H_2 gas without detections of H_2 in the individual J levels.

We find a conservative 3σ upper limit of $\log N(\text{H}_2) \lesssim 14.72 \text{ cm}^{-2}$ by adding the observed upper limits for the $J = 0$ and $J = 1$ levels to the theoretical upper limits (which are lower than the measured ones) calculated for the $J \geq 2$ levels from the $T = 1000$ K distribution. If the higher J levels were described by a more standard $T = 500$ K distribution (the other

dashed line in Fig. 3), the upper limit on the column density would be lower and equal to $\log N(\text{H}_2) \lesssim 14.55 \text{ cm}^{-2}$.

We derive a molecular hydrogen fraction of $f_{\text{H}_2} = 2N(\text{H}_2)/[N(\text{HI}) + 2N(\text{H}_2)] < 4.7 \times 10^{-7}$ by assuming the previously estimated values of $N(\text{HI}) = 2.2 \times 10^{21} \text{ cm}^{-2}$ and $N(\text{H}_2) < 5.25 \times 10^{14} \text{ cm}^{-2}$. The mass in H I of the cloud associated with the optical body of I Zw 18 (and probably completely included in the *FUSE* aperture) is $\sim 2.6 \times 10^7 M_\odot$ (van Zee et al. 1998b). This translates into an upper limit of $\sim 12 M_\odot$ for the total mass of diffuse H_2 in front of the sources of far-UV light in the galaxy. We cannot rule out that large amounts of clumpy molecular gas are present in I Zw 18. Clumpy H_2 has probably the same spatial distribution of dust (e.g., Cannon et al. 2002), considering that the major mechanism of H_2 formation is on the surface of dust grains. We do not simply see clumpy H_2 because the *FUSE* band selectively detects far-UV radiation passing through regions devoid of H_2 or intense enough to destroy H_2 molecules along the line of sight (Hoopes et al. 2003b).

7. Heavy Element Abundances

7.1. Column Densities

Table 2 lists interstellar absorption lines measured in the *FUSE* spectrum of I Zw 18 (see also Fig. 1). We cover several transitions of neutral and singly ionized atoms of heavy elements. Vacuum rest wavelengths λ_{lab} (column 2) of the transitions are from the compilation by Morton (1991). Oscillator strengths f (column 3) are from the references indicated in column 4. Rest-frame equivalent widths, W_0 , and their 1σ errors are listed in column 10. In a few cases where an interstellar line was found to be blended with another unrelated feature, its equivalent width is a lower limit that does not include the blend.

We derived values of column density for ions of interest by using the line-profile fitting technique (§ 3). The line profiles of most ions appear symmetric, and were simultaneously fitted by a single velocity component. The only exception is Fe II, where the asymmetric structure of its profile required the introduction of a second component in order to get an acceptable value for χ^2 . It is possible that an additional velocity component is well constrained for the Fe II lines only for the following reasons: *i*) there are many lines to consider for the fit; *ii*) the lines are quite faint, and the blend of the two components is less severe; *iii*) they are all located in the reddest part of the spectrum where the S/N is better. On the other hand, the fit with one component would give a similar iron column density within the uncertainties. In Table 2 we give the best-fit results for the ions considered: the redshift z is listed in column 5, the Doppler width b is reported in column 6, and the logarithm

of the column density N_{PF} is indicated in column 7. In the case of Fe II, we separately list the best fit parameters of both velocity components, as well as the total column density.

Fe II is the ion with the best constrained column density determination. Nine absorption lines with values of $f\lambda$ spanning a range of 25 from the weakest, $\lambda 1142$, to the strongest, $\lambda 1144$, were simultaneously considered to constrain the fit (Fig. 4). Moreover, we adopted recently updated values for the atomic oscillator strengths f that were empirically determined by Howk et al. (2000) in the *FUSE* band. Fe II $\lambda 1121$ from I Zw 18 is overlapping with Fe II $\lambda 1125$ from the HVC (Fig. 1), but other Fe II lines arising from the HVC indicate that this contamination is negligible. All the other metals considered in our analysis have less stringent constraints. For the ions of the α -elements O I, Si II, and Ar I, as well as for N I, a much smaller number of lines was available (Figs. 5 and 6). In other cases, such as the ions C I and P II, the absorption was not detected, and only an upper limit was inferred for the corresponding column density. Moreover, f -values from the older compilation by Morton (1991) were adopted for the transitions of these ions, the only exception being Ar I, for which we considered the newer values from Morton (2003, in preparation).

In the case of O I we used only two lines, $\lambda 976$ and $\lambda 1039$ (Fig. 5). All the other O I lines in the *FUSE* spectral range are contaminated, except for the very weak $\lambda 925$ that was not considered for the following reasons: *i*) the continuum placement is highly uncertain due to heavy contamination by other absorptions; *ii*) the S/N per resolution element is a factor of ~ 2 – 3 lower than for the other O I lines considered ($\lambda 976$ and $\lambda 1039$) due to the fact that $\lambda 925$ falls at the edge of the SiC 2A detector where the sensitivity is lower; *iii*) the oscillator strength has been only theoretically determined (see Morton 1991) and never empirically verified, since $\lambda 925$ has been rarely observed; moreover, some authors report problems associated with this line (e.g., Molaro et al. 2000; Hoopes et al. 2003a) and this could be an indication that the theoretical oscillator strength is wrong. We preferred not to use O I $\lambda 1302$ in the near-UV spectra of comparable resolution from HST/GHRS, since this spectrograph has a much smaller aperture sampling only a tiny region of I Zw 18 and spatial variations are expected within the galaxy (e.g., Brown et al. 2002). During the line-profile fitting procedure with the two selected O I lines ($\lambda 976$ and $\lambda 1039$) we noticed a degeneracy between column density N and Doppler parameter b . The weakest O I transition has a value of $f\lambda$ which is only 3 times lower than that of the strongest line. The degeneracy for O I is probably due to the instrumental resolution of FWHM ~ 35 km s $^{-1}$ coupled with the small range in $f\lambda$ values and probable partial saturation. We thus estimated the final column density and Doppler width of O I from line-profile fitting with the following procedure. We constrained the interval of possible values for both N and b from various acceptable fits, and we chose the center of the corresponding interval as our best estimate of a certain parameter and the half width of the same interval as the estimated uncertainty. The larger errors

associated with the oxygen column density and Doppler broadening reflect this procedure and are not related to statistical errors.

Different problems affect the column density determination of Si II. One of the two lines used for the fit, $\lambda 1020$, is partially blended with an H₂ line, and the continuum in that spectral region is slightly affected by the blue wing of Ly β (Fig. 5). The other line, $\lambda 989$, could be contaminated by N III $\lambda 989$. The absence of N II $\lambda 1083$ seems, however, to rule out this possibility (although the non-detection of this line could be partly due to poor S/N in the corresponding spectral region). On the other hand, the fit obtained by considering only Si II $\lambda 1020$ is consistent with the best fit from both absorptions (although with a slightly higher χ^2). This could be a further suggestion that contamination of the $\lambda 989$ line by N III is negligible. In the case of Si II we do not see the $N - b$ degeneracy problem, even if the strongest $\lambda 989$ line is partially saturated, and this is probably due to the fact that $f\lambda$ covers a wider range of values (the weakest transition has $f\lambda$ which is at least a factor of 4 lower than the strongest line).

Also the column density estimate of Ar I is more uncertain than for Fe II. The $\lambda 1048$ line is heavily blended with an H₂ line, and $\lambda 1066$ is very weak (Fig. 5). A large error is associated with the Doppler width of the Ar I ion. We have further investigated this issue with additional fits, and found out that b can vary over a large range of values, but the column density is always around the best fit estimate (Table 2).

Figure 6 presents the fit we obtained for N I. Only the two reddest lines of the 1134 triplet were used to this purpose, namely N I $\lambda 1134.4$ and N I $\lambda 1134.9$ for which we have a good constraint. N I $\lambda 1134.1$ was not considered for the fit due to its unusual shape. This probably arises from a local defect of the LiF 2A detector, whose data we considered in this wavelength range. The same feature is in fact weaker and shifted by one pixel ($\sim 0.04 \text{ \AA}$) in the lower S/N LiF 1B data covering the same spectral range. The two N I lines used are quite weak and not affected by saturation problems.

The ISM metal lines are found at velocities $v = z c$ that are consistent within the errors with the systemic velocity of $761 \pm 9 \text{ km s}^{-1}$ for the stellar component, after an uncertainty of $\delta v \lesssim 6 \text{ km s}^{-1}$ ($\delta\lambda \lesssim 0.02 \text{ \AA}$) from the fit centering is taken into account. The only exception is the second (reddest) component of Fe II with a velocity of $\sim 810 \text{ km s}^{-1}$. We want, however, to point out for consistency that the second Fe II component is well within the H I fit of all the Lyman series absorption lines considered (Fig. 2). An average value of $v = 764 \pm 6 \text{ km s}^{-1}$ is obtained from the ISM metal lines. This is consistent within the errors with the value of $753 \pm 6 \text{ km s}^{-1}$ we obtained for H I. We can finally assert that there is no evidence of a velocity shift between the absorption lines arising from heavy elements in the neutral ISM of I Zw 18 and its stellar features. This implies that on average there is no

evidence of gas outflow/infall over the large region of the galaxy sampled by *FUSE*.

The values of the Doppler width b that fit the ISM metal lines are all comparable, within the errors, to the instrumental broadening of $21 \pm 3 \text{ km s}^{-1}$. The only exceptions are the two velocity components of Fe II with $b \simeq 9$ and 3 km s^{-1} ($b \simeq 10 \text{ km s}^{-1}$ if only one component is considered for Fe II). Moreover, b seems to scale with the ion mass, once errors are correctly taken into account. Indeed the heavier ion Fe II has smaller b values than Si II, and the latter than the lighter ion N I. This trend resembles the case when thermal broadening is higher or comparable to turbulent broadening. Large uncertainties instead affect the b estimate of O I and Ar I. If we assume that also these ions behave consistently, we should have the Doppler parameter between ~ 16 and 19 km s^{-1} for O I and between ~ 10 and 16 km s^{-1} for Ar I. The line-profile fitting would give a column density of ~ 16.0 dex for O I if a mean value of $b \sim 18 \text{ km s}^{-1}$ is adopted, and a column density of ~ 13.6 dex for Ar I if a mean value of $b \sim 13 \text{ km s}^{-1}$ is considered. This is in agreement with what assumed in Table 2 for N_{PF} . However, we want again to point out that in the one- or two-velocity approximation models, b is an “effective” Doppler parameter with no real physical meaning (not simply related to turbulent and/or thermal broadening), since the observed absorption lines arise from the combination of many unresolved components.

In order to investigate the goodness of our single- or double-component approximations, we also performed the following test. We progressively added one velocity component at a time and fitted the Fe II lines. We were able to reasonably constrain up to 5 velocity components with b in the range $0.6 - 4 \text{ km s}^{-1}$. We observed, however, the following trend: the total column density is always consistent within 1σ with the value of 15.09 ± 0.06 dex of our best two-velocity component fit, even if the corresponding error increases with the number of velocity components (i.e., $\log N_{\text{PF}} = 15.25 \pm 0.14$ dex for five components).

We finally derived total column densities by applying the apparent optical depth method (§ 3) in order to discover hidden saturation in the unresolved components, as well as to test the one- or two-velocity approximation models with a measurement independent of the velocity structure of the absorbers. Column densities of I Zw 18 absorption lines estimated with this method are listed as N_{AOD} in column 9 of Table 2, the only exception being Si II $\lambda 989$, which is saturated (if $I_0(v)$ approaches 0, $\tau_a(v)$ becomes undetermined and the method is no longer applicable). Column 8 gives the velocity interval Δv over which equation (3) was calculated. By inspecting the values of N_{AOD} for Fe II, it is evident that the two strongest lines, $\lambda 1144$ and $\lambda 1063$, have a much lower apparent column density indicative of possible saturation. On the other hand, the average over the remaining transitions gives a value for N_{AOD} of 14.99 ± 0.14 dex, which is consistent within the errors with the value of N_{PF} . For O I, the lower value of N_{AOD} in the line $\lambda 1039$ suggests saturation problems. Nevertheless,

the other line, $\lambda 976$, gives a value for N_{AOD} of 15.96 ± 0.12 dex, which is in agreement with profile fitting measurements. The only unsaturated Si II line, $\lambda 1020$, is blended and the corresponding N_{AOD} is a lower limit consistent with our profile fitting measurements. Two lines are available for Ar I. The blended $\lambda 1048$ line gives a lower limit for the column density, while the weak $\lambda 1066$ line has a value of N_{AOD} in agreement with N_{PF} . N I has two absorptions that we used to infer the column density, and the mean value for N_{AOD} of 14.46 ± 0.05 dex is again consistent with the profile fitting results.

The application of the apparent optical depth method strengthens our assumption that in general the velocity models that we considered for the line-profile fitting are good representations of the *FUSE* data, even if the real physical situation is more complex. In the following, we will thus adopt N_{PF} for the final column densities of all ions in the neutral ISM of I Zw 18. However, we caution the reader that O I could be an exception. It is important to notice that the strengths of the O I lines differ by a factor of 3, yet there is still a 0.35 dex difference in N_{AOD} . The true O I column density may thus be underestimated by as much as 0.5 dex, if the apparent column densities listed in Table 2 are corrected for unresolved saturation as recommended by Savage & Sembach (1991). This would happen if the velocity distribution of the neutral gas contains very strong components that are substantially under-resolved by *FUSE*. Such an upward correction of the O I column density is still consistent within 2σ with the profile fitting results and would bring the O I abundance in the neutral gas up to a value closer to that in the H II regions. However, in the absence of additional information we will assume that the line-profile fitting and the apparent optical depth results for the weak line of O I ($\lambda 976$) give the correct column density for O I.

7.2. Abundance Determinations and Correction Effects

The major concern in abundance determinations from UV absorption-line analysis is represented by ionization and dust-depletion correction effects.

Ionization effects are usually neglected, and abundances are derived by assuming that the primary ionization state of an element in the neutral gas is representative of the total amount of the element. From Galactic interstellar studies it is well known that the singly ionized stage is the dominant one for most elements because their first ionization potential is below 13.6 eV (the H^0 ionization threshold) and their second one is above it. The neutral stage instead prevails for those elements having the first ionization potential above 13.6 eV. The reason for this is that the bulk of the H I gas with $N_{\text{HI}} \gtrsim 10^{19} \text{ cm}^{-2}$ is self-shielded from $h\nu > 13.6 \text{ eV}$ photons, but transparent to $h\nu < 13.6 \text{ eV}$ photons. This means that Fe II, C II, Si II, and P II, as well as O I, N I, and Ar I will be the dominant ionization stages of these

elements in the neutral gas of I Zw 18.

Some of the ions that are dominant ionization states in H I regions may also be produced in photoionized clouds where H I is a small fraction of the total hydrogen content. The formation of metal absorption lines in both ionized and neutral regions can have a significant impact on element abundance determinations. This problem has been recently tackled in detail for damped Ly α systems (DLAs) by Howk and Sembach (1999) and Vladilo et al. (2001) using the CLOUDY code (Ferland et al. 1998). These authors confirm previous findings that corrections to interstellar abundances are negligible for the majority of elements observed in DLAs in the case of high column densities, i.e. $N_{\text{HI}} \gtrsim 10^{21} \text{ cm}^{-2}$ (but see Prochaska et al. 2002, or Izotov et al. 2001 for a contrasting opinion on this issue). The ionization corrections are in general smaller when a stellar spectrum dominates over an external UV background as ionizing source of the ISM. This is the case in I Zw 18, where the radiation field is produced by its young massive stars.

The relative mixture of neutral and ionized gas contributing to an absorbing spectrum can be empirically determined by measuring adjacent ions of the same elements, e.g., Fe II/Fe III or Al II/Al III (Howk & Sembach 1999; Sembach et al. 2000; Prochaska et al. 2002). In the case of I Zw 18 we observed Fe III $\lambda 1122$. Fe III absorption is purely interstellar when a hot young O stellar population dominates the *FUSE* spectral range (Walborn et al. 2002; Pellerin et al. 2002), and only originates in the ionized gas associated with H II regions. The regions with neutral gas are instead where the bulk of Fe II absorption is produced. We followed the recipe of Sembach et al. (2000) to correct our derived Fe II abundances for ionization effects. Since the *FUSE* aperture integrates over a large area, we considered their “composite” model for the warm ionized ISM of the MW (a combination of overlapping low-excitation H II regions) as a better representation of the ionized gas conditions in I Zw 18. Unfortunately, Fe III $\lambda 1122$ is blended with Fe II $\lambda 1125$ from the MW and the HVC, but we could take this into account with the line-profile fitting. The total column density of Fe III we inferred from our measurements is 13.61 ± 0.08 dex (Fig. 7). This is also the Fe II contribution from the ionized gas, since half of the iron is in Fe III and half in Fe II (Table 5 of Sembach et al. 2000). This implies that $\lesssim 13.70$ dex of the total Fe II column density (15.09 ± 0.06 dex) measured in the *FUSE* spectra might be due to ionized gas, corresponding to an ionization fraction of at most 5%. If we correct for this factor, we get an Fe II column density in the neutral gas of 15.07 dex, just 0.02 dex lower than measured, and well within the 1σ errors. The radiation field is likely to be much higher in I Zw 18 than in the MW thanks to the higher density of younger and hotter stars responsible for it. In addition, the ISM metallicity in I Zw 18 is much lower than in the MW, this property implying higher temperatures for the gas since less heavy elements are available for cooling. Both effects go in the direction of favoring more iron in the Fe III ionization state than in the

Fe II, thus much lower ionization corrections. For example, if we consider for our model a higher ionization parameter of $\log(q) = -2$ instead of the value of -4 of the MW, we obtain that $\sim 70\%$ (and not 50%) of the iron is Fe III, corresponding to an ionization fraction less than 2% . Fe III is thus a very good tracer of ionized gas (much better than Al III), since it is the dominant state of iron for a wide range of ionizing conditions (e.g., effective temperature of the ionizing central star or ionization parameter).

The ionization correction for Fe II is one of the largest: in the ionized gas all the other elements like H, O, N, and Ar are found mostly ($\gtrsim 80\%$) in an ionization state higher (II) than the one we detect in the UV spectra (I). We can thus assess that ionization effects should be negligible in our *FUSE* data. The only exception is Si, where as much as $\sim 90\%$ of Si II (70% for a more plausible higher ionization parameter of $\log(q) = -2$) could arise in the ionized gas. However, no absorption lines of Si III are available in the *FUSE* band to correctly take this into account.

The presence of dust in the ISM can represent another serious complication in the interpretation of the metal abundances. Refractory elements (e.g., Fe and Si) are more easily locked into dust grains than non-refractory ones (e.g., O, Ar, N). This can clearly alter the total heavy element abundances. Observations of the local ISM provide hints of selective depletions acting in dense clouds within our Galaxy (Savage & Sembach 1996). There is evidence of dust also in the DLAs, systems that I Zw 18 resembles in its H I column density. The reddening of QSOs lying behind DLA absorption is a clear clue of dust extinction (Pei, Fall, & Bechtold 1991; Fall & Pei 1993). Evidence of elemental depletion similar to that observed in the nearby ISM was first reported for DLAs by Pettini et al. (1994), and further supported by others (Hou, Boissier, & Prantzos 2001; Prochaska & Wolfe 2002), although with a much lower dust-to-gas ratio (typically $\sim 1/30$) than in our own Galaxy (Pettini et al. 2000). Molecular hydrogen has also been found recently in 15% - 20% of a sample of DLAs and usually in those systems with the highest metallicities and largest dust depletions (Ledoux, Petitjean, & Srianand 2003). On the contrary, I Zw 18 does not show detectable H_2 .

A detailed study of the dust content of I Zw 18 from its H II regions has been performed recently by Cannon et al. (2002). A bidimensional map of the extinction has been obtained from the ratio between $H\alpha$ and $H\beta$ HST/WFPC2 images. The optical extinction, A_V , varies significantly from one region to another, suggesting a patchy dust distribution, but the extinction is always small, with a maximum value of ~ 0.5 mag and a mean value of only ~ 0.15 mag. This is not an unexpected trend, since low-metallicity galaxies should have a lower and more patchy dust content (Morgan & Edmunds 2003).

Dust traced by emission-line spectra does not necessarily correspond to dust content in

the neutral ISM (different geometries and different regions are involved). This is the reason why it is important to have an indication of depletion directly from our *FUSE* absorption measurements. The same methods applied to DLAs could be used for this purpose. In general, dust properties are often assumed to be similar to those of the Galactic interstellar dust, and the amount of depletion is simply scaled by taking into account variations of the dust-to-metal ratios (Vladilo 1998; Savaglio 2001). However, the observed abundances arise from the combination of *i*) a non-solar nucleosynthesis, *ii*) a non-solar star-formation history, and *iii*) a certain dust depletion pattern. In order to disentangle these effects, refractory and non-refractory elements originating from similar nucleosynthetic histories should be considered in the analysis, i.e., the Fe-peak group (e.g., Cr, Zn and Fe). Unfortunately, only the Fe abundance has been measured in the neutral ISM of I Zw 18.

In the absence of a possible measurement of the dust content in the neutral ISM of I Zw 18, we will not consider depletion corrections in our following analysis. This is clearly an approximation, but we do not expect significant corrections due to the very low metal content of the galaxy. Moreover, among all the chemical elements considered, only Si and Fe are sensitive to this problem. For reference, in DLAs the depletion corrections can be as high as ~ 0.2 – 0.4 dex for Si, and ~ 0.7 – 1.1 dex for Fe (Garnett 2002). We note that we can use oxygen and argon (neither of which will be depleted) to determine the abundances of the α elements.

In Table 3 we summarized the column densities of ions representative of the total amount of an element in the neutral phase of the ISM (column 3). Only an upper limit is available for P II. C I ($\log N < 14.40$ at 3σ level) was omitted, since C II is the dominant state for carbon. However, the only C II absorption line in the *FUSE* spectral range, $\lambda 1036$, is heavily contaminated by O I $\lambda 1039$ from the MW. This implies that we were unable to determine the carbon abundance in the neutral ISM of I Zw 18. Column densities were converted into abundances relative to $N(\text{H})$ by adopting the standard solar photospheric abundances published by Grevesse, Noels, & Sauval (1996), and the formula $[X/\text{H}] = \log(X/\text{H}) - \log(X/\text{H})_{\odot}$ (column 6). The only exception is oxygen, for which an updated solar value of $12 + \log(\text{O}/\text{H}) = 8.69 \pm 0.05$ dex (~ 0.2 dex lower than previously believed) from Allende Prieto, Lambert, & Asplund (2001) was used. Errors on $[X/\text{H}]$ reflect measurement errors in $N(X)$. For a direct comparison, column 7 and 8 of Table 3 present abundances for the ionized gas in the northwest (NW) and southeast (SE) H II regions of I Zw 18. These have been homogenized to the neutral gas abundances by rescaling the values from Izotov et al. (1999) and Izotov and Thuan (1999) with our adopted solar scale. In this way, the oxygen abundance of the H II regions turns out to be $\sim 1/33$ solar compared to the old value of $\sim 1/50$.

8. Discussion

8.1. Comparison with Abundances in the H II Regions

Our *FUSE* observations sample absorption lines of three α -elements, O, Ar and Si. Oxygen in the H II regions is the most secure abundance measurement of all the elements whose ions have been detected in the different ISM phases of I Zw 18. On the other hand, oxygen in the neutral gas phase has the highest uncertainty, and could be affected by systematic errors that could increase its abundance by as much as ~ 0.5 dex (§ 7.1). However, if we take our estimate at face value, we infer for the neutral ISM an $[\text{O}/\text{H}] = -2.06 \pm 0.28$ dex, which is ~ 3 – 4 times lower than in the ionized gas (Table 3). A similar trend is found for oxygen in the BCD Mrk 59 by Thuan et al. (2002). The difference between H I and H II regions (if not related to systematic uncertainties) cannot be explained with ionization effects in the neutral gas, since O I is tightly related to H I, so that $[\text{O I}/\text{H I}] = [\text{O}/\text{H}]$. It cannot be explained with dust depletion either, since O is non-refractory, and it can only be the result of nucleosynthesis.

The argon abundance in the H II regions of I Zw 18 is on average $[\text{Ar}/\text{H}] = -1.51 \pm 0.08$ dex, a factor of ~ 6 times higher than the value measured in the neutral ISM (Table 3). Part of the difference between neutral and ionized gas could be due to ionization effects. Ar does not generally behave like H (and O) in the ISM despite similar ionization potentials (Sofia & Jenkins 1998; Jenkins et al. 2000). Its larger photoionization cross section renders much easier for Ar to hide in its ionized form, Ar II, if photons with $h\nu > 15.76$ eV (the Ar I ionization threshold) are able to leak through a H I layer (i.e., low column density regions with $N(\text{H I}) \lesssim 10^{19} \text{ cm}^{-2}$). As a result the $[\text{Ar I}/\text{H I}]$ ratio is lower than the real $[\text{Ar}/\text{H}]$. However, due to the relatively high column densities of the ISM, we expect ionization effects to be negligible in I Zw 18. If ionization is not important, we should observe the same value of $\log(\text{Ar}/\text{O})$ in the different gas phases of I Zw 18, since both Ar and O are non-refractory and are produced by the same stars. And indeed the value of $\log(\text{Ar}/\text{O}) = -2.16 \pm 0.08$ dex for the ionized gas seems to be preserved within the errors in the neutral phase, where $\log(\text{Ar}/\text{O}) = -2.38 \pm 0.27$ dex, in agreement with the predictions of standard stellar nucleosynthesis models (e.g., Woosley & Weaver 1995). The $\log(\text{Ar}/\text{O})$ ratio of I Zw 18 is well within the range (-2.00 to -2.5) found in both low (van Zee, Haynes, & Salzer 1997) and high (Thuan, Izotov, & Lipovetsky 1995) surface brightness star-forming dwarf galaxies. It is also interesting that the Ar/O ratio in the neutral gas of I Zw 18 (as well as in its H II regions) has practically a solar value ($[\text{Ar}/\text{O}] = -0.21 \pm 0.31$ dex), and is very similar to the interstellar value of $[\text{Ar}/\alpha] \sim -0.2$ dex estimated by Vladilo et al. (2003) for the local universe.

The other α -element, silicon, behaves in a slightly different manner. Its abundance of $[\text{Si}/\text{H}] = -2.09 \pm 0.12$ dex in the neutral ISM is only marginally lower than in the H II regions (Table 3). Depletion cannot explain the lack of a clear Si excess in the H II regions (even if it can justify a lower Si content compared to the other α -elements). Dust grains are more easily destroyed (than formed) by star-formation through shocks generated by supernova explosions and propagating into the ISM (Savage & Sembach 1996). The following possibilities must instead be considered: *i*) our abundance is overestimated due to contamination problems affecting the Si II lines (§ 7.1); *ii*) ionization corrections are not negligible for this element, at variance with what we assumed (§ 7.2), and the real abundance in the neutral gas is lower than inferred; *iii*) the abundances in the H II regions are higher than reported (note the large uncertainties given in Table 3); *iv*) part of the Si in the neutral gas has been produced by SNe Ia, not just SNe II, even if this contribution should be small. On the other hand, we cannot completely rule out that the different ISM phases are more homogeneous than indicated by the other α -elements, O and Ar.

The iron abundance in the neutral ISM of I Zw 18 is one of our most reliable estimates. On the other hand, the Fe content in the southeast H II region (Izotov et al. 1999) is likely more uncertain than suggested by the formal error of Table 3 (0.09 dex). The iron abundance is derived from a single Fe^{2+} emission line ($[\text{Fe III}] \lambda 4658$), but most of the iron is in Fe^{3+} . Thus, an ionization correction factor (ICF) has to be applied in order to infer the total amount of this element from its minority species. It is possible that the ICF value is more uncertain than quoted (the authors do not formally report any error). This is suggested, e.g., by the scatter of the ICF for different regions of the other BCD analyzed in the same article, SBS 0335-052. The Fe content in the neutral ISM of I Zw 18 is, however, consistent, within the uncertainties, with that in the ionized gas. Iron, thus, behaves differently from the α -elements O and Ar, whose abundances are several times lower in the neutral gas, and more similarly to the third α -element considered, Si.

The last element directly comparable in H I and H II regions is nitrogen. The value of $[\text{N}/\text{H}] = -2.88 \pm 0.11$ we derived for the neutral gas in I Zw 18 is a factor of ~ 3 lower than in the southeast H II region. Ionization (but not depletion) effects could be responsible for part of this difference, since for $N(\text{H I}) \lesssim 10^{19} \text{ cm}^{-2}$ N I is not strongly coupled to H I and behaves more similarly to Ar I, even if to a smaller extent (Sofia & Jenkins 1998; Jenkins et al. 2000). However, in the nearby starburst galaxy NGC 1705, where $N(\text{H I}) \simeq 10^{20} \text{ cm}^{-2}$, Heckman et al. (2001) were able to directly address this issue with detections of both N I and N II, and indeed they found that most of the observed N II must be associated with the warm photoionized gas. In our case, we do not detect N II $\lambda 1083$ (§ 7.1), so we expect ionization effects to be negligible. In addition, we also note that the solar value of Ar/O in both the neutral and ionized ISM of I Zw 18 rules out ionization effects for Ar

in the H I region, and this is an even stronger result for N. We thus conclude that the N underabundance in the neutral ISM of I Zw 18, compared to its H II regions, is real and only due to stellar nucleosynthesis.

8.2. The Chemical Evolutionary History of I Zw 18

What can we infer about the evolutionary state of I Zw 18 from the metal content of its interstellar gas? The first straightforward conclusion is that the abundances of heavy elements in its neutral ISM are low, but not zero: α -elements are between $\sim 1/100$ and $1/200$ solar, Fe is $\sim 1/60$ solar, and N is $\sim 1/800$ solar. According to Panagia (2002), a metallicity above $10^{-3} Z_{\odot}$ for elements arising from SNe II (i.e., α -elements) is the result of one or more episodes of metal enrichment. This implies that the neutral gas in I Zw 18 has already been enriched with the products of at least one star-formation event, and is not primordial in nature. However, its extremely low abundances do not leave much room for a large amount of star-formation.

The abundance pattern we observe in the different gaseous components of I Zw 18 directly leads to a second conclusion. The metal content is significantly lower in the H I than in the H II regions, apart from iron which is the same. The α -elements are mainly produced by SNe II on short time scales (less than 50 Myr), while iron is mostly released by SNe Ia on time scales longer than 1 Gyr. This may indicate that the H II regions, compared to the neutral ISM, have been additionally enriched in α -elements (and nitrogen) by more recent star formation activity.

Can we invoke self-enrichment of the H II regions by their massive stars? In general, the concept of self-enrichment (Kunth & Sargent 1986) does not agree with the homogeneity observed in H II regions in dwarf star-forming galaxies (e.g., Kobulnicky & Skillman 1997). I Zw 18 is not an exception from this point of view (Skillman & Kennicutt 1993; Vílchez & Iglesias-Parámo 1998; Legrand et al. 2000). In addition, Larsen, Sommer-Larsen, & Pagel (2001) present theoretical evidence that the supershells triggered by SNe II and stellar winds from massive stars are always well within the H II regions for almost the whole existence of these regions (less than 10 Myr). This implies that elements newly synthesized in an ongoing burst are trapped in the hot phase of these superbubbles and can never be well mixed with the emitting gas within the H II region. It is thus highly unlikely that we are witnessing direct self-enrichment in the H II regions of I Zw 18.

A key element for shedding light on the chemical evolution of I Zw 18 is nitrogen. The nature and origin of nitrogen in galaxies has been debated for a long time. In massive

metal-rich galaxies, N/O increases roughly linearly with O/H (Torres-Peimbert, Peimbert, & Fierro 1989; van Zee, Salzer, & Haynes 1998a). This is the typical behavior for “secondary” nitrogen, produced by intermediate-mass stars on time scales longer than $\sim 250 - 300$ Myr. In contrast, dwarf star-forming galaxies (Thuan et al. 1995; Kobulnicky & Skillman 1996; van Zee et al. 1997) and low-metallicity H II regions in spirals (van Zee et al. 1998a) show a relatively constant N/O *versus* O/H with the plateau around $\log(\text{N/O}) = -1.5$. This is attributed to “primary” nitrogen, mainly produced by intermediate-mass stars (Renzini & Voli 1981; Meynet & Maeder 2002a), but also by low-metallicity massive ($M > 30 M_{\odot}$) stars (Woosley & Weaver 1995; Meynet & Maeder 2002b) on much shorter time scales (~ 10 Myr). The nitrogen abundance in I Zw 18 is higher in the H II regions than in the neutral ISM, consistent with what is found for α -elements. This indicates that there has been metal enrichment by star formation that occurred long enough ago for primary nitrogen to have been released back into the ISM. This dates the star formation to at least ~ 10 Myr ago (if massive stars are responsible), or several hundred Myr ago (if intermediate-mass stars are responsible). The simplest interpretation would be that the current episode of star-formation traced by the H II regions has been going on long enough for nitrogen enrichment to have occurred in this part of the galaxy ISM.

We can place time constraints on the different star-formation episodes with simple considerations of the physical scales involved. The nucleosynthetic activity responsible for the enrichment in the H II regions must have taken place long enough ago for gas mixing to be efficient in the central optical part of the galaxy (as testified by the homogeneity of the H II regions; Izotov et al. 1999). The linear scales involved are around ~ 0.5 kpc, corresponding to mixing time scales of ~ 100 Myr (Roy & Kunth 1995). It must have also started recently enough so that mixing on physical scales comparable to the extended H I envelope surrounding the star-forming regions is incomplete. The halo of I Zw 18 is ~ 5 kpc wide from H I maps of van Zee et al. (1998b). This corresponds to mixing time scales around ~ 1 Gyr (Tenorio-Tagle 1996). We thus conclude that the star-formation process responsible for the additional enrichment of the H II regions must have started more recently than 1 Gyr ago and have been active for at least a hundred Myr. This rules out contribution to primary nitrogen only from massive stars with very short lifetimes (~ 10 Myr). By the same reasoning, the ancient star-formation episode responsible for the metals in the H I must have started at least ~ 1 Gyr ago to allow for diffusion of metals from the central stellar production sites.

The times of the various star-formation activities can be further constrained by considering the behavior of abundance ratios involving elements produced on different time scales. One of the most powerful tools from this point of view is O/Fe. According to Gilmore & Wyse (1991), at the beginning of the very first star-formation activity we should find a value of $[\text{O/Fe}] \simeq +0.63$ dex ($+0.45$ on the old oxygen solar scale) which reflects the relative pro-

duction of O and Fe from a mean SN II. As soon as the first SNe Ia start to explode, this ratio begins to decrease due to additional Fe contributions. The decrement is more rapid in the case of a short burst than for continuous star-formation. The onset of another burst will simultaneously, and almost instantaneously, increase the contribution to the ISM of both O and Fe from SNe II. The O/Fe ratio will suddenly jump to a higher value, even if always lower than the initial value due to the continuous contribution from SNe Ia to Fe only. In the neutral ISM of I Zw 18 we infer a value of $[O/Fe] = -0.30 \pm 0.30$. This clearly indicates a substantial Fe enrichment from SNe Ia in the H I gas, and ages longer than 1 Gyr for the oldest episode. On the other hand, a supersolar value of $[O/Fe] = +0.45 \pm 0.09$ is found in the southeast H II region, where the Fe/H ratio (a metallicity indicator) is instead the same within the errors. This implies that more recent and relatively young star-formation activity (with no contribution from additional SNe Ia, thus with an age less than 1 Gyr) is responsible for the further enrichment of the ionized gas. The epochs we infer by analyzing the behavior of O/Fe are thus in agreement with our considerations of the mixing processes for both the ancient and more recent star-formation episodes.

The O/Fe results on the age of the ancient star-formation activity are quite strong. They are still valid even if iron is partly depleted onto dust grains, since the contribution from SNe Ia would be higher in this case. Also infall of primordial gas (e.g., Matteucci & Chiosi 1983; Edmunds 1990) would not alter this conclusion, as its net effect would be the dilution of the whole metal content and would not affect relative abundances. What could influence these findings is the presence of gas outflow, especially if it is selectively enriched in α -elements from SNe II (Pilyugin 1993; Marconi, Matteucci, & Tosi 1994; Bradamante, Matteucci, & D’Ercole 1998; Recchi et al. 2002; but see also Recchi, Matteucci, & D’Ercole 2001 for an alternative enrichment in iron from SNe Ia). The loss of oxygen through galactic winds would decrease the O/Fe ratio in a way that could mimic the iron contribution from SNe Ia. However, our *FUSE* data provide no observational evidence of a gas outflow in I Zw 18. Martin (1996) discusses the existence of a bipolar H α bubble with a dynamical age of 15–30 Myr that will eventually evolve into a galactic wind. This does not imply that part of the ISM has already been ejected from the galaxy. From their analysis of the O VI $\lambda\lambda 1032, 1038$ doublet, Heckman et al. (2002) find no indication of a “warm” coronal phase associated with I Zw 18, although this could reflect the very low oxygen abundance. The lack of large-scale outflows in the early stages of I Zw 18 evolution is theoretically predicted by Recchi et al. (2002). In their chemical evolution model, a galactic wind enriched in SNe II products sets in only in the last 15 Myr with the second and more intense of two bursts of star formation.

Under the assumption of no gas outflow, we calculated the number of SNe Ia that have enriched the neutral ISM of I Zw 18. The following procedure was applied. The Fe abundance

in the H I gaseous component probably arises from both SNe II and SNe Ia. We disentangled their relative contribution by taking into account the quantity of oxygen produced by SNe II during the star-formation event and the prescriptions by Gibson, Loewenstein, & Mushotzky (1997). This amounts to $\sim 50\%$ for SNe Ia and $\sim 50\%$ for SNe II in the case of $[\text{O}/\text{Fe}] = -0.30$ (-0.12 on the old oxygen solar scale). We obtained a total Fe mass of $\sim 700 M_{\odot}$ by assuming a total H I mass of $\sim 2.6 \times 10^7 M_{\odot}$ (van Zee et al. 1998b) and an Fe abundance equal to $\sim 1/60$ solar ($[\text{Fe}/\text{H}] = -1.76$). Only $\sim 50\%$ of this mass has been produced by SNe Ia. Considering a typical SN Ia yield of $\sim 0.74 M_{\odot}$ for iron (Gibson et al. 1997), we inferred that ~ 470 SNe Ia are required in order to justify the metal enrichment in the neutral ISM of I Zw 18.

The N/O ratio can also help us in further investigating the nature and properties of the star-formation activity in I Zw 18. Unlike the Fe ratio, N/O is free of dust depletion. Moreover, in the case of I Zw 18 ionization problems do not affect its value since N I should behave like O I (see § 8.1). We have already mentioned the existence of a plateau in the N/O *versus* O/H relation for metal-poor star-forming galaxies and its explanation as being due to primary nitrogen. Many authors (Edmunds & Pagel 1978; Garnett 1990; Larsen et al. 2001; Contini et al. 2002; Chiappini, Romano, & Matteucci 2003) are able to reproduce this plateau with their chemical evolution models by simply considering a bursting regime coupled to the time delay between the delivery into the ISM of O from massive stars and N from intermediate-mass stars. Primary nitrogen from massive stars is thus not a necessary condition, at variance with the early suggestions by Izotov and Thuan (1999). On the other hand, Henry, Edmunds, & Köppen (2000) propose a more continuous low-level ($\sim 10^{-3} M_{\odot} \text{ yr}^{-1} \text{ kpc}^{-2}$) of star-formation activity to justify the existence of the plateau. This last model is more consistent with the picture that BCDs have an underlying old (several Gyr) metal-poor stellar population with bursts superimposed on it (e.g., the chemical evolution model of I Zw 18 by Legrand 2000). Every galaxy that evolves slowly will thus maintain a relatively low metallicity over a significant fraction of a Hubble time since the total metallicity is directly related to the star-formation rate integrated over time. Values of $\log(\text{N}/\text{O})$ well below the plateau, as observed in some DLAs (Lu, Sargent, & Barlow 1998; Centurión et al. 2003), can be found only in the very early stages of the N/O evolution, when the stellar objects have ages younger than or comparable to the typical time scales for the release of primary N from intermediate-mass stars (Henry et al. 2000; Centurión et al. 2003).

From our *FUSE* observations we obtain a value of $\log(\text{N}/\text{O}) = -1.54 \pm 0.26$ for $\log(\text{O}/\text{H}) = -5.37 \pm 0.28$. The neutral ISM of I Zw 18 thus follows the flat trend in N/O *versus* O/H observed for dwarf star-forming galaxies (e.g., Garnett 2002), as well as metal-rich DLAs (Centurión et al. 2003). However, it is well above the values found at similar metallicities in those O-poor DLAs considered to be chemically young systems (Lu

et al. 1998; Centuri3n et al. 2003). Hence, H I gas in I Zw 18 seems to have been polluted by star-formation at least as old as the typical lag time (250–300 Myr) for N released by intermediate-mass stars, and probably older than 1 Gyr (based on the results for O/Fe). A value of $\log(N/O) = -1.57 \pm 0.06$ for $\log(O/H) = -4.82 \pm 0.03$ is inferred for the southeast H II region of I Zw 18. Such a similar N/O but a higher O content in the ionized gas compared to the neutral ISM are possible only if the galaxy is experiencing or has experienced additional star-formation which has released additional oxygen from SNe II but also additional nitrogen from massive or intermediate-mass stars.

Silicon is the last element that we can consider to constrain the star-formation history of I Zw 18. It is an α -element produced mainly by SNe II, but behaves differently from O and Ar (see § 8.1). For example, Si is depleted onto dust grains in studies of the local ISM, while Ar and O are non-refractory (Savage & Sembach 1996). Izotov & Thuan (1999) have, however, found that Si/O is constant with O/H in their sample of BCDs, and claimed that the similarity of this plateau with the solar value is evidence of no depletion in the H II regions. Silicon is also more affected by ionization corrections than O and Ar, since Si II is the majority species in intervening H II gas as well. Moreover, a small amount of silicon is produced by SNe Ia (Matteucci, Molaro, & Vladilo 1997), at variance with the other α -elements considered in our analysis. The silicon abundance in the neutral gas of I Zw 18 is similar to the oxygen one. On the other hand, Si in the H II regions is lower than the other α -elements. Two interpretations are possible to explain these observations: *i*) the Si value in the ionized gas is higher than estimated; *ii*) Si is depleted in the H II regions, and as a consequence in the neutral gas as well; however, no depletion is noticed in the neutral ISM because ionization is important for Si II or some contribution from SNe Ia is present. In general, silicon tracks very well the other α -elements O and S, so that $O/Si \simeq S/Si \simeq 0$ (indicative of the same SNe II origin). This is, e.g., what is observed in dwarf star-forming galaxies (Izotov & Thuan 1999) and DLAs (Prochaska & Wolfe 1999; Vladilo et al. 2003). Thus, the first interpretation is probably the one to prefer since $[O/Si] = +0.03 \pm 0.30$ in the neutral ISM of I Zw 18.

Summarizing, the chemical evolutionary history of I Zw 18 suggests that the galaxy has experienced at least two star-formation events. Ancient activity (one or more star-formation episodes) is responsible for the metal enrichment of the H I gaseous component. The imprinting of the chemical elements produced by SNe Ia is clearly detectable in this component, as inferred by the O/Fe ratio. A probable age of at least ~ 1 Gyr can be inferred for this ancient star-formation event. More recent activity is instead accountable for the higher metal content in the H II regions. It is more difficult to confine in time the extension of this stellar production. However, some constraints arise from the abundance patterns in the neutral and ionized gas. According to our findings, this event must be

younger than ~ 1 Gyr (no additional Fe enrichment in the H II regions), but old enough to have enriched the gas in the central optical portion of the galaxy with primary nitrogen. This minimum age is 10 Myr or a few hundred Myr, depending on the source of primary nitrogen (massive or intermediate-mass stars). The scenario of a few hundred Myr is favored from considerations of time scales of mixing processes in the ISM.

9. Summary and Conclusions

We have presented our analysis of the interstellar spectrum of I Zw 18, the most metal-poor star-forming galaxy in the local universe. The new *FUSE* observations, with a spectral resolution of ~ 35 km s $^{-1}$, have higher S/N and better coverage of the wavelength region 900–1200 Å than previous observations. Our main findings are as follows.

1. We have studied the absorption lines of the H I Lyman series from Ly β to Ly η . These lines are narrow in shape suggesting a purely interstellar origin, with no significant stellar contamination. A column density of $2.2_{-0.5}^{+0.6} \times 10^{21}$ cm $^{-2}$ is inferred for H I in I Zw 18 by a multi-component fitting technique.

2. No H $_2$ lines are detected in I Zw 18. We have set a conservative 3σ upper limit of 5.25×10^{14} cm $^{-2}$ for the total column density of diffuse H $_2$. This very low limit does not exclude the possible presence of clumpy H $_2$ in dusty compact star-forming regions that are opaque to far-UV radiation.

3. Many interstellar absorption lines of neutral and singly ionized atoms of heavy elements have been detected and analyzed. Fe II is the ion with the best column density constraint which is based on 9 lines with different oscillator strengths. Column density determinations of other ions, O I, Si II, Ar I, and N I, have also been made.

4. From the kinematics of the absorption lines, there is no clear evidence of gas in-fall/outflow over the large region sampled by *FUSE*. All the lines are centered at a velocity consistent with the systemic velocity of the galaxy as inferred by its stellar component ($v_{\text{stars}} = 761 \pm 9$ km s $^{-1}$).

5. The single- or two-velocity component models used in the multi-component fitting technique have turned out to be a quite good representation of the data when compared to the column densities inferred with the optical depth method. The “effective” Doppler width of the different ions is around 20 km s $^{-1}$, similar to our instrumental broadening.

6. We have inferred the following abundances of heavy elements: $[\text{Fe}/\text{H}] = -1.76 \pm 0.12$, $[\text{O}/\text{H}] = -2.06 \pm 0.28$, $[\text{Si}/\text{H}] = -2.09 \pm 0.12$, $[\text{Ar}/\text{H}] = -2.27 \pm 0.13$, and $[\text{N}/\text{H}] =$

– 2.88 ± 0.11 . Ionization and dust depletion corrections have been considered and should be small. The neutral ISM in I Zw 18 has thus been enriched in metals by a certain amount of star-formation.

7. A direct comparison of metal abundances in the neutral and ionized gas of I Zw 18 indicates that the α -elements (O, Ar, and Si) and N are several times lower in the neutral ISM, while the Fe content is the same within the errors. This suggests that the H II regions have been enriched by additional star-formation.

8. The analysis of the abundance ratios O/Fe, N/O and O/Si and simple considerations of gas mixing, have allowed us to put some constraints on the chemical evolutionary history of I Zw 18. It seems highly plausible that this galaxy has experienced two separate star-formation events. Ancient star-formation activity (one or more episodes) is responsible for the metal enrichment of the H I gas with the products typical of SNe Ia. An age of at least ~ 1 Gyr can thus be inferred. We estimated that the number of SNe Ia required to produce the Fe content in the neutral ISM is ~ 470 . It is more difficult to confine in time the extension of the more recent star-formation activity responsible for the higher metal content in the H II regions. If primary N is released by intermediate-mass (metal-poor massive) stars, then the enrichment requires several hundred Myr (10 Myr). The older age seems to be preferred by typical time scales related to mixing processes. In either case, the time scales are longer than the typical lifetime of H II regions ($\lesssim 10$ Myr).

It is worth noting that the simple scenario we inferred from the abundance patterns in the different gaseous components of I Zw 18, is consistent with the star-formation history derived for this galaxy from the optical/NIR color-magnitude diagrams of its resolved stellar population (Aloisi et al. 1999; Östlin 2000). These diagrams revealed for the first time the existence of single stars with ages around 1 Gyr, and the study presented in this paper seems to suggest the detection of their chemical imprinting in the neutral ISM of the galaxy.

We can conclude that I Zw 18 seems to be a dwarf star-forming galaxy which has substained a stellar-production activity for quite a long time, despite its very low metallicity. This activity has probably occurred with a low star-formation rate and/or relatively long quiescent periods. Hence, I Zw 18 is just a relatively old galaxy with a very slow chemical evolution. This scenario is in agreement with the recent findings that all star-forming dwarf galaxies resolved into single stars show a stellar production that has gone on for quite a large fraction of a Hubble time with a so-called “gasp” star-formation regime (Tosi 2001).

Acknowledgements The authors thank William van Dixon, Alex Fullerton, and Ravi Sankrit for their help in the calibration and spectral reduction of FUSE data. Fabrizio Brighenti, Thomas Brown, Annibale D’Ercole, Sally Oey, Livia Origlia, Nino Panagia, Si-

mone Recchi, Monica Tosi, Giovanni Vladilo, René Walterbos, and Rosemary Wyse are also acknowledged for stimulating discussion about I Zw 18 and the chemical evolution of dwarf star-forming galaxies. We also thank Max Pettini, Evan Skillman, and Kim Venn for their careful reading of the manuscript and their helpful suggestions for a more balanced paper. An anonymous referee is also acknowledged for his/her comments which contributed to improve the paper. This work is based on observations made with the NASA-CNES-CSA *FUSE* mission operated for NASA by the Johns Hopkins University under NASA contract NAS5-32985. Financial support has been provided by NASA Long Term Space Astrophysics grants NAG5-6400 and NAG5-3485.

REFERENCES

- Abgrall, H., & Roueff, E. 1989, *A&AS*, 79, 313
- Allende Prieto, C., Lambert, D. L., & Asplund, M. 2001, *ApJ*, 556, L63
- Aloisi, A., Tosi, M., & Greggio, L. 1999, *AJ*, 118, 302
- Babul, A., & Rees, M. J. 1992, *MNRAS*, 255, 346
- Bradamante, F., Matteucci, F., & D’Ercole, A. 1998, *A&A*, 337, 338
- Brown, T. M., Heap, S. R., Hubeny, I., Lanz, T., & Linder, D. 2002, *ApJ*, 579, L75
- Cannon, J. M., Skillman, E. D., Garnett, D. R., & Dufour, R. J. 2002, *ApJ*, 565, 931
- Cayrel, R. 1996, *A&A Rev.*, 7, 217
- Centurión, M., Molaro, P., Vladilo, G., Péroux, C., Levshakov, S. A., & D’Odorico, V. 2003, *A&A*, 403, 55
- Chiappini, C., Romano, D., & Matteucci, F. 2003, *MNRAS*, 339, 63
- Contini, T., Treyer, M. A., Sullivan, M., & Ellis, R. S. 2002, *MNRAS*, 330, 75
- Dekel, A., & Silk, J. 1986, *ApJ*, 303, 39
- De Mello, D. F., Schaerer, D., Heldmann, J., & Leitherer, C. 1998, *ApJ*, 507, 199
- De Young, D. S., & Heckman, T. M. 1994, *ApJ*, 431, 598
- Dufour, R. J., Garnett, D. R., & Shields, G. A. 1988, *ApJ*, 332, 752

- Edmunds, M. G. 1990, MNRAS, 246, 678
- Edmunds, M. G., & Pagel, B. E. J. 1978, MNRAS, 185, 78
- Fall, S. M., & Pei, Y. C. 1993, ApJ, 402, 479
- Ferland, G. J., Korista, K. T., Verner, D. A., Ferguson, J. W., Kinkgdon, J. B., & Verner, E. M. 1998, PASP, 110, 761
- Fontana, A., & Ballester, P. 1995, The ESO Messenger, 80, 37
- Garnett, D. R. 1990, ApJ, 363, 142
- Garnett, D. R. 2002, in Cosmochemistry: the Melting Pot of the Elements, ed. C. Esteban, A. Herrero, R. García López, & F. Sánchez, in press, astro-ph/0211148
- Garnett, D. R., Dufour, R. J., Peimbert, M., Torres-Peimbert, S., Shields, G. A., Skillman, E. D., Terlevich, E., & Terlevich, R. J. 1995a, ApJ, 449, L77
- Garnett, D. R., Skillman, E. D., Dufour, R. J., Peimbert, M., Torres-Peimbert, S., Terlevich, R., Terlevich, E., & Shields, G. A. 1995b, ApJ, 443, 64
- Garnett, D. R., Skillman, E. D., Dufour, R. J., & Shields, G. A. 1997, ApJ, 481, 174
- Gibson, B. K., Loewenstein, M., & Mushotzky, R. F. 1997, MNRAS, 290, 623
- Gilmore, G., & Wyse, R. F. G. 1991, ApJ, 367, L55
- Gondhalekar, P. M., Johansson, L. E. B., Brosch, N., Glass, I. S., & Brinks, E. 1998, A&A, 335, 152
- González-Delgado, R. M., Leitherer, C., & Heckman, T. 1997, ApJ, 489, 601
- Grevesse, N., Noels, A., & Sauval, A. J. 1996, in ASP Conference Series 99, Cosmic Abundances, ed. S. S. Holt, & G. Sonneborn, 117
- Heckman, T. M., Norman, C. A., Strickland, D. K., & Sembach, K. R. 2002, ApJ, 577, 691
- Heckman, T. M., Sembach, K. R., Meurer, G. R., Strickland, D. K., Martin, C. L., Calzetti, D., & Leitherer, C. 2001, ApJ, 554, 1021
- Henry, R. B. C., Edmunds, M. G., & Köppen, J. 2000, ApJ, 541, 660
- Hobbs, L. M. 1974, ApJ, 191, 395

- Hoopes, C. G., Sembach, K. R., Hébrard, G., Moos, H. W., & Knauth, D. C. 2003a, *ApJ*, 586, 1094
- Hoopes, C. G., Sembach, K. R., Heckman, T. M., Meurer, G. R., Aloisi, A., Calzetti, D., Leitherer, C., & Martin, C. L. 2003b, *ApJ*, submitted
- Hou, J. L., Boissier, S., & Prantzos, N. 2001, *A&A*, 370, 23
- Howk, J. C., & Sembach, K. R. 1999, *ApJ*, 523, L141
- Howk, J. C., Sembach, K. R., Roth, K. C., & Kruk, J. W. 2000, *ApJ*, 544, 867
- Hunt, L. K., Thuan, T. X., & Izotov, Y. I. 2003, *ApJ*, 588, 281
- Ikeuchi, S., & Norman, C. A. 1987, *ApJ*, 312, 485
- Izotov, Y. I., Chaffee, F. H., Foltz, C. B., Green, R. F., Guseva, N. G., & Thuan, T. X. 1999, *ApJ*, 527, 757
- Izotov, Y. I., Schaerer, D., & Charbonnel, C. 2001, *ApJ*, 549, 878
- Izotov, Y. I., & Thuan, T. X. 1999, *ApJ*, 511, 639
- Jenkins, E. B. 1986, *ApJ*, 304, 739
- Jenkins, E. B., Oegerle, W. R., Gry, C., Vallergera, J., Sembach, K. R., Shelton, R. L., et al. 2000, *ApJ*, 538, L81
- Kniazev, A. Y., Pustilnik, S. A., Masegosa, J., Márquez, I., Ugryumov, A. V., Martin, J. M., Izotov, Y. I., Engels, D., Brosch, N., Hopp, U., Merlino, S., & Lipovetsky, V. A. 2000, *A&A*, 357, 101
- Kobulnicky, H. A., & Skillman, E. D. 1996, *ApJ*, 471, 211
- Kobulnicky, H. A., & Skillman, E. D. 1997, *ApJ*, 489, 636
- Kudritzki, R. P. 2002, *ApJ*, 577, 389
- Kunth, D., Lequeux, J., Sargent, W.L.W., & Viallefond, F. 1994, *A&A*, 282, 709
- Kunth, D., & Sargent, W. L. W. 1986, *ApJ*, 300, 496
- Kurucz, R. L. 1979, *ApJS*, 40, 1
- Larsen, T. I., Sommer-Larsen, J., & Pagel, B. E. J. 2001, *MNRAS*, 323, 555

- Ledoux, C., Petitjean, P., & Srianand, R. 2003, MNRAS, submitted, astro-ph/0302582
- Legrand, F. 2000, A&A, 354, 504
- Legrand, F., Kunth, D., Roy, J.-R., Mas-Hesse, J. M., & Walsh, J. R. 2000, A&A, 355, 891
- Lequeux, J., & Viallefond, F. 1980, A&A, 91, 269
- Levshakov, S. A., Kegel, W. H., & Agafonova, I. I. 2001, A&A, 373, 836
- Lu, L., Sargent, W. L. W., & Barlow, T. A. 1998, AJ, 115, 55
- Lu, L., Sargent, W. L. W., Barlow, T. A., Churchill, C. W., & Vogt, S. S. 1996, ApJS, 107, 475
- Marconi, G., Matteucci, F., & Tosi, M. 1994, MNRAS, 270, 35
- Marlowe, A. T., Heckman, T. M., Wyse, R. F. G., & Schommer, R. 1995, ApJ, 438, 563
- Martin, C. L. 1996, ApJ, 465, 680
- Martin, C. L., Kobulnicky, H. A., & Heckman, T. M. 2002, ApJ, 574, 663
- Marzke, R. O., & da Costa, L. N. 1997, AJ, 113, 185
- Mas-Hesse, J. M., & Kunth, D. 1999, A&A, 349, 765
- Matteucci, F., & Chiosi, C. 1983, A&A, 123, 121
- Matteucci, F., Molaro, P., & Vladilo, G. 1997, A&A, 321, 45
- Meurer, G. R., Heckman, T. M., & Calzetti, D. 1999, ApJ, 521, 64
- Meynet, G., & Maeder, A. 2002a, A&A, 381, L25
- Meynet, G., & Maeder, A. 2002b, A&A, 390, 561
- Molaro, P., Bonifacio, P., Centurión, M., D’Odorico, S., Vladilo, G., Santin, P., & Di Marcantonio, P. 2000, ApJ, 541, 54
- Moos, H. W., Cash, W. C., Cowie, L. L., Davidsen, A. F., Dupree, A. K., Feldman, P. D., et al. 2000, ApJ, 538, L1
- Morgan, H. L., & Edmunds, M. G. 2003, MNRAS, submitted, astro-ph/0302566
- Morton, D. C. 1991, ApJS, 77, 119

- Östlin, G. 2000, *ApJ*, 535, L99
- Panagia, N. 2002, ASP Conference Series, *Origins 2002: The Heavy Element Trail from Galaxies to Habitable Worlds*, ed. C. E. Woodward & E. P. Smith, in press, *astro-ph/0209346*
- Pei, Y. C., Fall, S. M., & Bechtold, J. 1991, *ApJ*, 378, 6
- Pellerin, A., Fullerton, A. W., Robert, C., Howk, J. C., Hutchings, J. B., Walborn, N. R., Bianchi, L., Crowther, P. A., & Sonneborn, G. 2002, *ApJS*, 143, 159
- Persic, M., Mariani, S., Cappi, M., Bassani, L., Danese, L., Dean, A. J., et al. 1998, *A&A*, 339, 33
- Petrosian, A. R., Boulesteix, J., Comte, G., Kunth, D., & LeCoarer, E. 1997, *A&A*, 318, 390
- Pettini, M., Ellison, S. L., Steidel, C. C., Shapley, A. E., & Bowen, D. V. 2000, *ApJ*, 532, 65
- Pettini, M., & Lipman, K. 1995, *A&A*, 297, L63
- Pettini, M., Rix, S. A., Steidel, C. C., Adelberger, K. L., Hunt, M. P., & Shapley, A. E. 2002, *ApJ*, 569, 742
- Pettini, M., Smith, L. J., Hunstead, R. W., & King, D. L. 1994, *ApJ*, 426, 79
- Pilyugin, L. S. 1993, *A&A*, 277, 42
- Prochaska, J. X., Howk, J. C., O’Meara, J. M., Tytler, D., Wolfe, A. M., Kirkman, D., Lubin, D., & Suzuki, N. 2002, *ApJ*, 571, 693
- Prochaska, J. X., & Wolfe, A. M. 1999, *ApJ*, 121, 369
- Prochaska, J. X., & Wolfe, A. M. 2002, *ApJ*, 566, 68
- Prochaska, J. X., Wolfe, A. M., Tytler, D., Burles, S., Cooke, J., Gawiser, E., Kirkman, D., O’Meara, J. M., & Storrie-Lombardi, L. 2001, *ApJS*, 137, 21
- Recchi, S., Matteucci, F., & D’Ercole, A. 2001, *MNRAS*, 322, 800
- Recchi, S., Matteucci, F., D’Ercole, A., & Tosi, M. 2002, *A&A*, 384, 799
- Renzini, A., & Voli, M. 1981, *A&A*, 94, 175
- Robert, C., Pellerin, A., Aloisi, A., Leitherer, C., Hoopes, C., & Heckman, T. M. 2003, *ApJS*, 144, 21

- Roy, J. R., & Kunth, D. 1995, *A&A*, 294, 432
- Savage, B. D., & Sembach, K. R. 1991, *ApJ*, 379, 245
- Savage, B. D., & Sembach, K. R. 1996, *ARA&A*, 34, 279
- Savaglio, S. 2001, in *IAU Symp. 204, The Extragalactic Infrared Background and its Cosmological Implications*, ed. M. Harwit & M. G. Hauser, (San Francisco: ASP) 307
- Searle, L., & Sargent, W. L. W. 1972, *ApJ*, 173, 25
- Sembach, K. R., Howk, J. C., Ryans, R. S. I., & Keenan, F. P. 2000, *ApJ*, 528, 310
- Sembach, K. R., Howk, J. C., Savage, B. D., & Shull, J. M. 2001, *AJ*, 121, 992
- Shull, J. M., & Beckwith, S. 1982, *ARA&A*, 20, 163
- Skillman, E. D. 1998, in *Stellar Astrophysics for the Local Group*, ed. A. Aparicio, A. Herrero, & F. Sánchez (Cambridge: Cambridge Univ. Press), 457
- Skillman, E. D., & Kennicutt, R. C. 1993, *ApJ*, 411, 655
- Sofia, U. J., & Jenkins, E. B. 1998, *ApJ*, 499, 951
- Spitzer, L. 1978, *Physical Processes in the Interstellar Medium* (New York: John Wiley)
- Spitzer, L., Cochran, W. D., & Hirshfeld, A. 1974, *ApJS*, 28, 373
- Stark, A. A., Gammie, C. F., Wilson, R. W., Bally, J., Linke, R. A., Heiles, C., & Hurwitz, M. 1992, *ApJS*, 79, 77
- Tenorio-Tagle, G. 1996, *AJ*, 111, 1641
- Thuan, T. X. 1991, in *Massive Stars in Starbursts*, ed. C. Leitherer, N. R. Walborn, T. M. Heckman, & C. A. Norman (Cambridge: Cambridge Univ. Press), 183
- Thuan, T. X., Izotov, Y. I., & Lipovetsky, V. A. 1995, *ApJ*, 445, 108
- Thuan, T. X., Izotov, Y. I., Lipovetsky, V. A., & Pustilnik, S. A. 1994, in *ESO/OHP Workshop on Dwarf Galaxies*, ed. G. Meylan & P. Prugniel (Garching: ESO), 421
- Thuan, T. X., Lecavelier des Etangs, A., & Izotov, Y. I. 2002, *ApJ*, 565, 941
- Thuan, T. X., Lipovetsky, V. A., Martin, J.-M., & Pustilnik, S. A. 1999, *A&AS*, 139, 1
- Thuan, T. X., & Martin, G. E. 1981, *ApJ*, 247, 823

- Torres-Peimbert, S., Peimbert, M., & Fierro, J. 1989, *ApJ*, 345, 186
- Tosi, M. 2001, in *Dwarf Galaxies and their Environment*, ed. K. S. de Boer, R. J. Dettmar, & U. Klein (Shaker Verlag), 67
- van Zee, L., Haynes, M. P., & Salzer, J. J. 1997, *AJ*, 114, 2497
- van Zee, L., Salzer, J. J. , & Haynes, M. P. 1998a, *ApJ*, 497, L1
- van Zee, L., Westpfahl, D., Haynes, M. P., & Salzer, J. J. 1998b, *AJ*, 115, 1000
- Viallefond, F., Lequeux, J., & Comte, G. 1987, in *Starbursts and Galaxy Evolution*, ed. T. X. Thuan, T. Montmerle, & J. Tran Thanh Van, (Gif-sur-Yvette: Edition Frontières), 139
- Vidal-Madjar, A., Kunth, D., Lecavelier des Etangs, A., Lequeux, J., André, M., BenJaffel, L. et al. 2000, *ApJ*, 538, L77
- Vílchez, J. M., & Iglesias-Páramo, J. 1998, *ApJ*, 508, 248
- Vladilo, G. 1998, *ApJ*, 493, 583
- Vladilo, G., Centurión, M., Bonifacio, P., & Howk, J. C. 2001, *ApJ*, 557, 1007
- Vladilo, G., Centurión, M., D’Odorico, V., & Péroux, C. 2003, *A&A*, 402, 487
- Walborn, N. R., Fullerton, A. W., Crowther, P. A., Bianchi, L., Hutchings, J. B., Pellerin, A., Sonneborn, G., & Willis, A. J. 2002, *ApJS*, 141, 443
- Welsh, B. Y., Rachford, B. L., & Tumlinson, J. 2002, *A&A*, 381, 566
- White, S. D. M., & Rees, M. J. 1978, *MNRAS*, 183, 341
- Woosley, S. E., & Weaver, T. A. 1995, *ApJS*, 101, 181

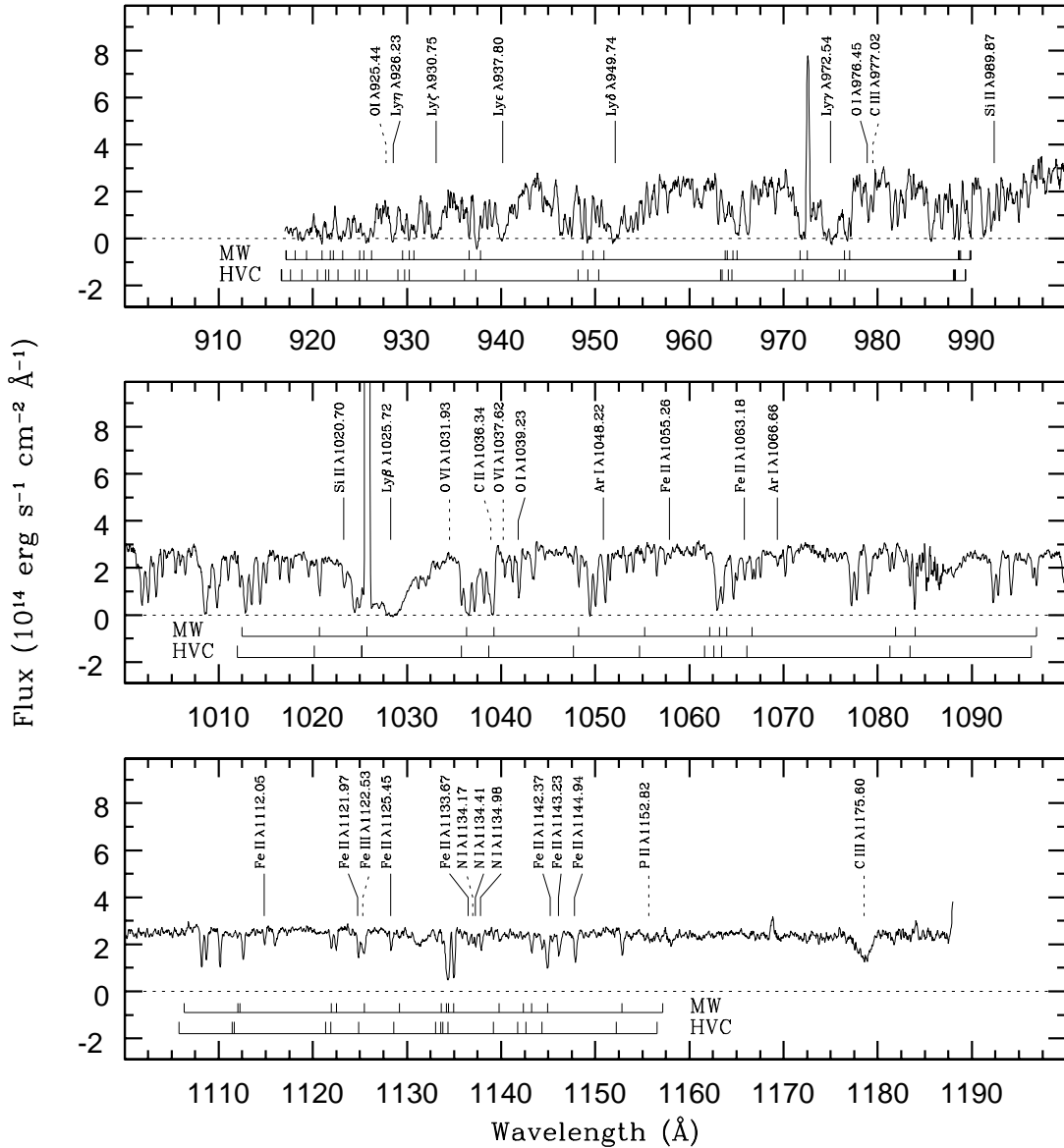


Fig. 1.— I Zw 18 *FUSE* spectrum in the range 917–1188 \AA . The data have been smoothed by a 5-point boxcar. Uncontaminated interstellar absorption lines at $v \simeq 750 \text{ km s}^{-1}$ used in the determination of metal abundances are indicated with solid lines. Other interstellar/stellar absorptions associated with the galaxy and discussed in our analysis are marked with dotted lines. The ticks indicate the position of all low-ionization interstellar absorption lines (see Prochaska et al. 2001 for a compilation) that could potentially arise from the Milky Way (MW) at $v = 0 \text{ km s}^{-1}$ or the well known high-velocity cloud (HVC) at $v = -160 \text{ km s}^{-1}$. Unmarked strong absorption lines below 1120 \AA are due to molecular hydrogen from the ISM of the Milky Way (I Zw 18 does not show detectable H_2).

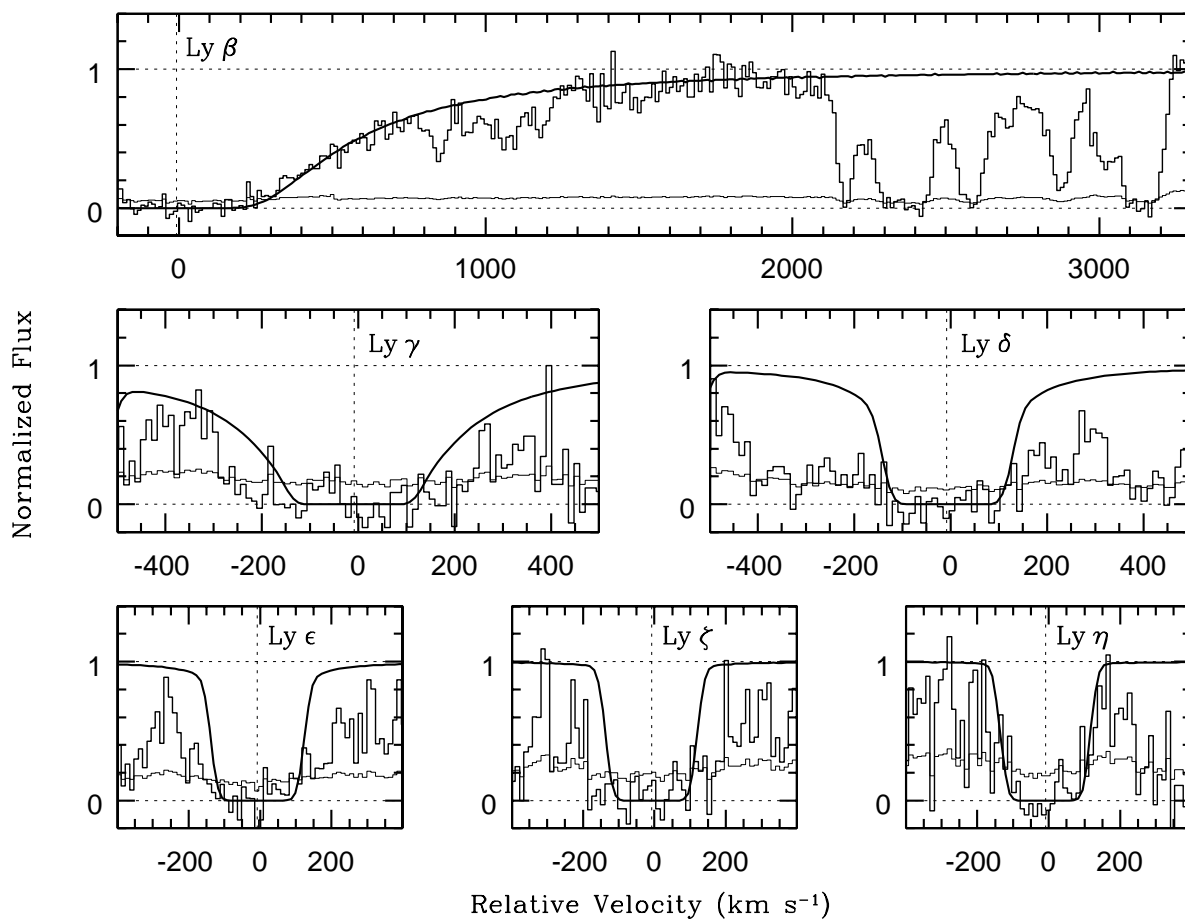


Fig. 2.— H I Lyman series profiles in I Zw 18. Observed spectrum (*histogram*) and theoretical line profile for $N = 2.2 \times 10^{21} \text{ cm}^{-2}$ and $b = 35 \text{ km s}^{-1}$ at $v = 753 \text{ km s}^{-1}$ (*solid line*). The velocity scale is relative to $v_{\text{stars}} = 761 \text{ km s}^{-1}$. The spectrum of the noise per pixel is also shown (*thin line histogram*).

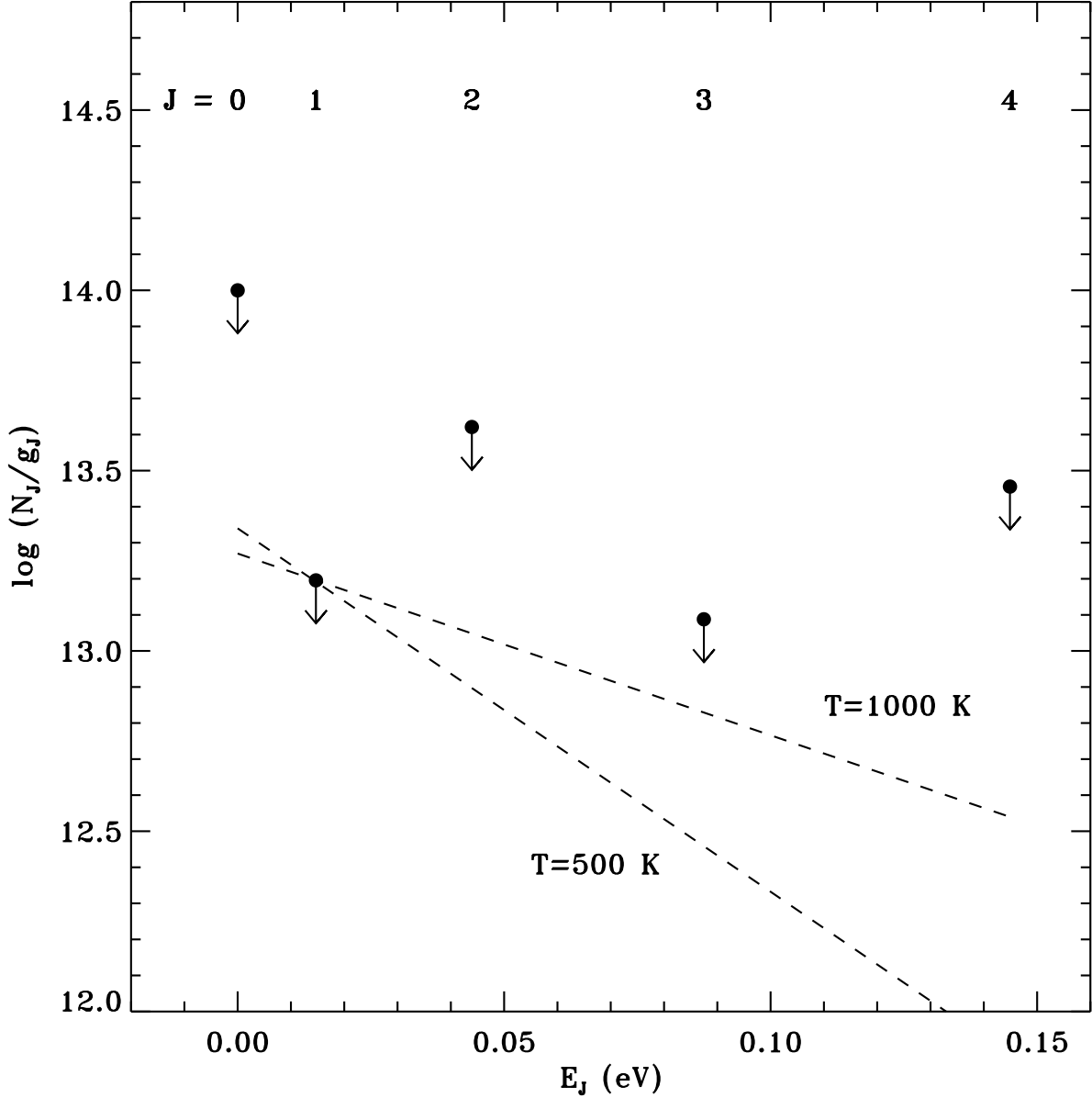


Fig. 3.— Excitation diagram for H_2 intrinsic to I Zw 18. The column density N_J divided by the statistical weight g_J is plotted *versus* the excitation potential E_J for each J level. The points are 3σ upper limits on the H_2 column densities derived from the strongest unblended transition for each of the first 5 rotational levels. The dashed lines are Boltzmann distributions for excitation temperatures of $T = 500$ and 1000 K. These are *assumed* temperatures used to improve the upper limit on the total H_2 column density. We cannot constrain the excitation temperature with the upper limits we have measured.

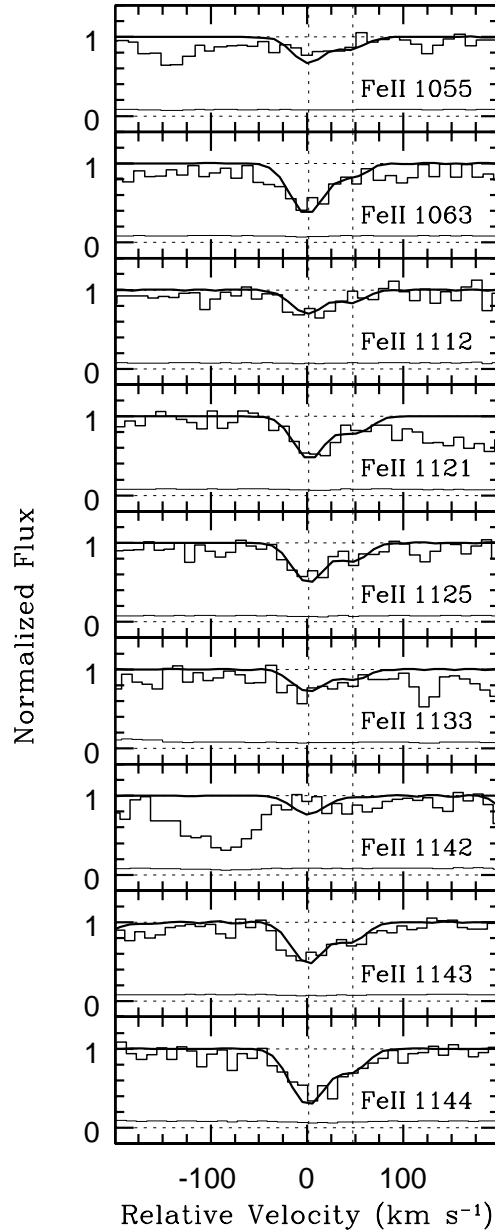


Fig. 4.— Fe II profiles in I Zw 18: observed spectrum (*histogram*) and theoretical line profile (*solid line*). A two-velocity component model has been used: $N_1 = 1.0 \times 10^{15} \text{ cm}^{-2}$ and $b_1 = 8.8 \text{ km s}^{-1}$ at $v_1 = 764 \text{ km s}^{-1}$ for the first component; $N_2 = 2.3 \times 10^{14} \text{ cm}^{-2}$ and $b_2 = 3.2 \text{ km s}^{-1}$ at $v_2 = 809 \text{ km s}^{-1}$ for the second component. The velocity scale is relative to $v_{\text{stars}} = 761 \text{ km s}^{-1}$. The spectrum of the noise per pixel is also shown (*thin line histogram*).

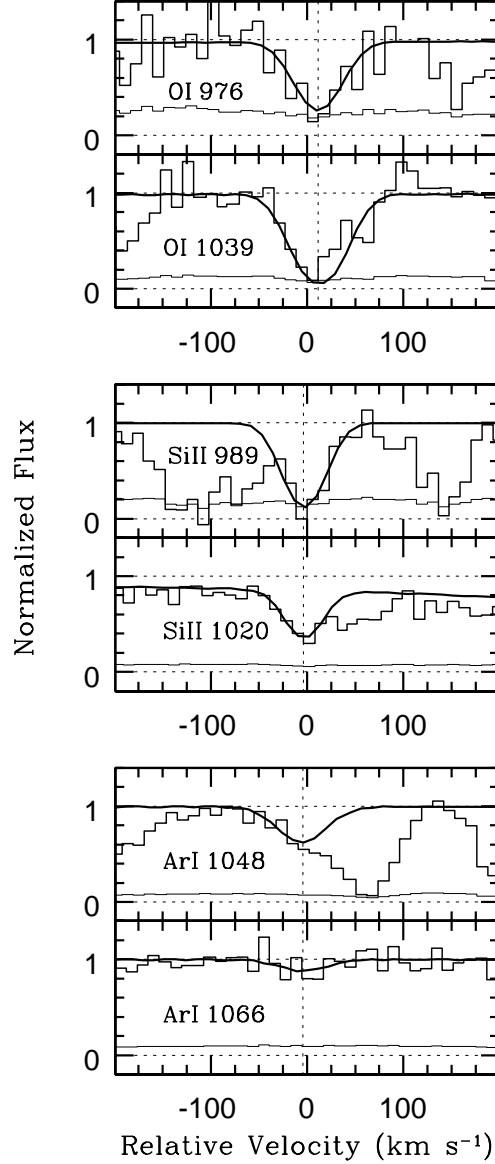


Fig. 5.— Same as Fig. 4, but for the α -elements. A single-velocity component has been fitted to the data with the following parameters: $N = 9.5 \times 10^{15} \text{ cm}^{-2}$ and $b = 23 \text{ km s}^{-1}$ at $v = 774 \text{ km s}^{-1}$ for O I (top panel); $N = 6.5 \times 10^{14} \text{ cm}^{-2}$ and $b = 15.7 \text{ km s}^{-1}$ at $v = 758 \text{ km s}^{-1}$ for Si II (middle panel); $N = 4.0 \times 10^{13} \text{ cm}^{-2}$ and $b = 27 \text{ km s}^{-1}$ at $v = 757 \text{ km s}^{-1}$ for Ar I (bottom panel). The absorptions contaminating Si II $\lambda 1020$ and Ar I $\lambda 1048$ are from H_2 in the ISM of the Milky Way and have been independently modelled.

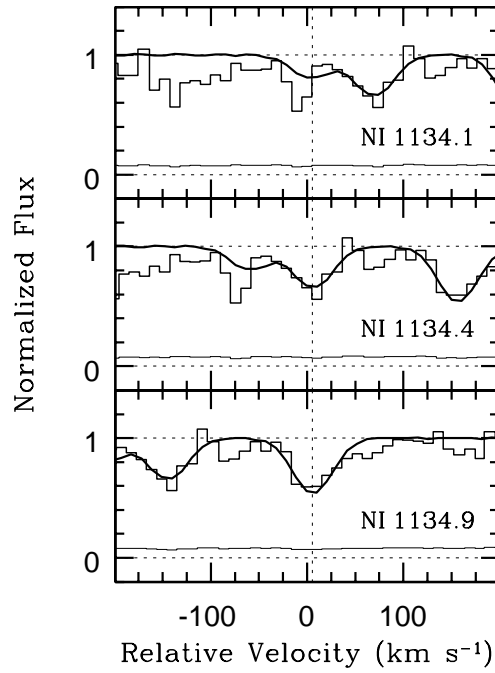


Fig. 6.— Same as Fig. 4, but for N I. Again, a single-velocity component has been modeled with the following parameters: $N = 2.8 \times 10^{14} \text{ cm}^{-2}$ and $b = 19 \text{ km s}^{-1}$ at $v = 768 \text{ km s}^{-1}$. N I $\lambda 1134.1$ is the bluest line of the 1134 triplet: it has not been considered to constrain the fit parameters due to its unusual shape (artifact/defect of the detector?), but it is shown here for completeness.

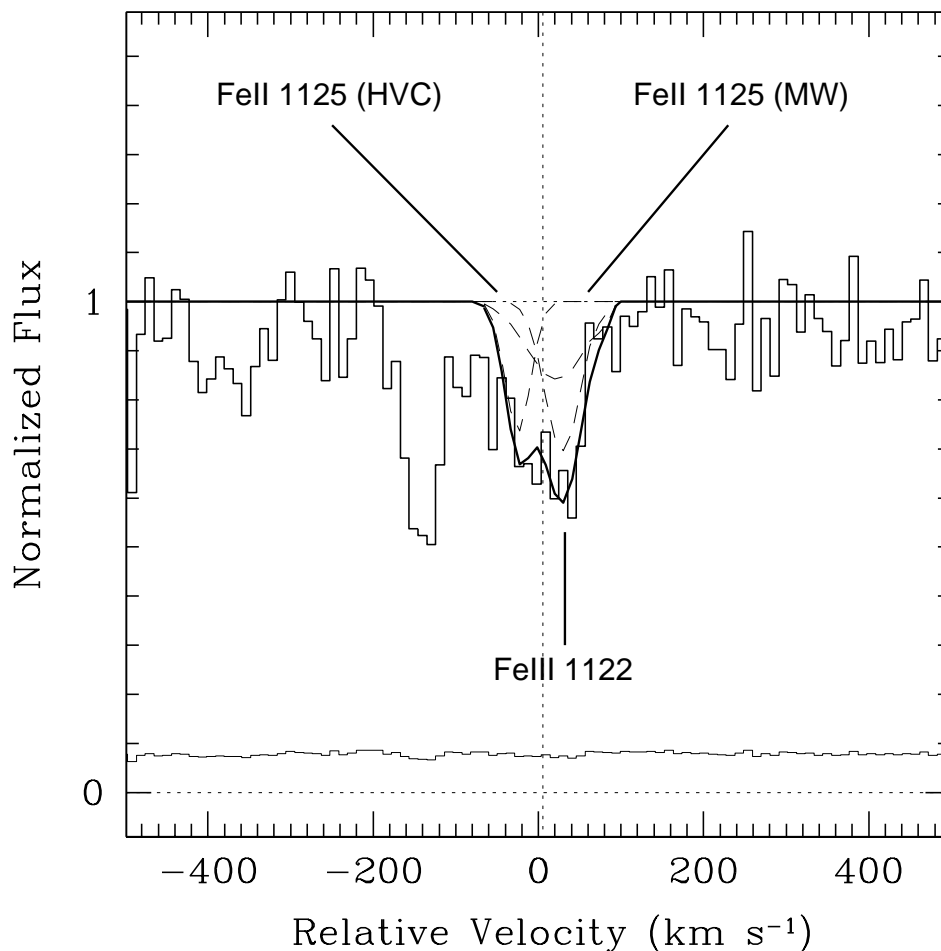


Fig. 7.— Fit of the Fe III absorption line arising from I Zw 18: observed spectrum (*histogram*) and theoretical line profiles (*solid and dashed lines*). Fe III (deep dashed line on the right) is blended with Fe II $\lambda 1125$ from the MW (shallow dashed line on the right) and the HVC (deep dashed line on the left). The solid line represents the composite fit. The contaminating absorption features were well constrained by simultaneous line-profile fitting of other uncontaminated Fe II lines from, respectively, the MW and the HVC at different wavelengths. A final column density of $N = 4.0 \times 10^{13} \text{ cm}^{-2}$ was derived for the Fe III line. The spectrum of the noise per pixel is also shown (*thin line histogram*).

Table 1. Parameters for H₂ intrinsic to I Zw 18

Level	Line ID	λ_{lab} (Å)	$\log(f\lambda)$ ^a	W_0 ^b (mÅ)	N_J ^c (cm ⁻²)
$J = 0$	(7–0) R(0)	1012.817	1.483	< 27.5	< 1.0×10^{14}
$J = 1$	(7–0) R(1)	1013.441	1.307	< 25.7	< 1.4×10^{14}
$J = 2$	(4–0) R(2)	1051.498	1.168	< 28.4	< 2.1×10^{14}
$J = 3$	(7–0) R(3)	1017.427	1.263	< 44.0	< 2.6×10^{14}
$J = 4$	(6–0) R(4)	1032.351	1.244	< 41.6	< 2.6×10^{14}

^aWavelengths and oscillator strengths from Abgrall & Roueff (1989).

^bRest-frame equivalent width. Upper limits are 3σ .

^cColumn density. Upper limits are 3σ .

NOTE.— Lines in this table are those providing the most stringent limits to the inferred column densities in each J level.

Table 2. Interstellar Absorption Lines associated with I Zw 18

Ion	$\lambda_{\text{lab}}^{\text{a}}$ (Å)	f^{b}	Ref.	PROFILE FITTING			APPARENT OPTICAL DEPTH		W_0 (mÅ)
				z	b (km s ⁻¹)	$\log N_{\text{PF}}$ (cm ⁻²)	Δv (km s ⁻¹)	$\log N_{\text{AOD}}$ (cm ⁻²)	
Fe II ^c	1055.262	0.0075	2	0.0025462	8.81 ± 0.47	15.00 ± 0.05	- 40 to + 80	14.91 ± 0.09	56 ± 9
				0.0026983	3.21 ± 0.38	14.37 ± 0.10			
				15.09 ± 0.06 ^d			
	1063.176	0.05998	1				- 40 to + 80	14.21 ± 0.07	80 ± 13
	1112.048	0.0062	2				- 40 to + 80	15.12 ± 0.06	78 ± 10
	1121.975 ^e	0.0202	2				- 40 to + 80	14.82 ± 0.04	119 ± 11
	1125.448	0.016	2				- 40 to + 80	14.85 ± 0.04	110 ± 11
	1133.665	0.0055	2				- 40 to + 80	15.23 ± 0.05	100 ± 11
	1142.366	0.0042	2				- 40 to + 80	15.10 ± 0.09	22 ± 8
1143.226	0.0177	2				- 40 to + 80	14.92 ± 0.04	145 ± 11	
1144.938	0.106	2				- 40 to + 80	14.28 ± 0.03	175 ± 11	
O I ^f	976.448 ^g	0.003300	1	0.0025786	23.00 ± 8.00	15.98 ± 0.26	- 40 to + 80	15.96 ± 0.12	158 ± 31
	1039.230	0.009197	1				- 40 to + 80	15.61 ± 0.05	207 ± 13
Si II	989.873 ^h	0.1330	1	0.0025264	15.71 ± 2.85	14.81 ± 0.07	137 ± 17 ⁱ
	1020.699 ^j	0.02828	1				- 40 to + 30	14.70 ± 0.05 ^k	84 ± 7 ⁱ
Ar I	1048.220 ^l	0.263	3	0.0025246	27.02 ± 12.88	13.60 ± 0.08	- 40 to + 15	13.53 ± 0.05 ^k	78 ± 8 ⁱ
	1066.660	0.0675	3				- 40 to + 80	13.64 ± 0.20	29 ± 11
N I	1134.415	0.02683	1	0.0025587	19.05 ± 4.83	14.44 ± 0.04	- 40 to + 80	14.51 ± 0.06	69 ± 9
	1134.980	0.04023	1				- 40 to + 80	14.41 ± 0.05	101 ± 10

^aVacuum wavelengths from Morton (1991).

^bOscillator strengths from references indicated in column 4.

^cFit with two velocity components.

^dTotal column density of the two velocity components.

^eOverlapping with HVC Fe II λ 1125, but contamination negligible.

^fLine-profile fitting values of N_{PF} and b for O I (and relative uncertainties) are to be intended as central value of an interval of possible values (and relative half width). See § 7.1 for more details.

^gContinuum slightly affected by red wing of Ly γ .

^hPossible blend with N III λ 989.

ⁱEquivalent width is a lower limit due to partial blend

^jBlend with H₂, continuum affected by blue wing of Ly β .

^kColumn density from the apparent optical depth method N_{AOD} is a lower limit.

^lBlend with H₂.

Table 3. Interstellar Abundances in I Zw 18

Element	Ion	$\log N$	$\log (X/H)$	$\log (X/H)_{\odot}$ ^a	$[X/H]$ ^b	$[X/H]_{\text{HII}}$ ^c	
						NW	SE
H	H I	21.35 ± 0.10
Fe	Fe II	$15.09 \pm 0.06^{\text{d}}$	-6.26 ± 0.12	-4.50	-1.76 ± 0.12	...	-1.96 ± 0.09
O	O I	15.98 ± 0.26	-5.37 ± 0.28	-3.31	-2.06 ± 0.28	-1.52 ± 0.03	-1.51 ± 0.03
Si	Si II	14.81 ± 0.07	-6.54 ± 0.12	-4.45	-2.09 ± 0.12	-1.94 ± 0.23	-1.86 ± 0.23
Ar	Ar I	13.60 ± 0.08	-7.75 ± 0.13	-5.48	-2.27 ± 0.13	-1.43 ± 0.05	-1.58 ± 0.05
N	N I	14.44 ± 0.04	-6.91 ± 0.11	-4.03	-2.88 ± 0.11	...	-2.36 ± 0.07
P	P II	$< 13.60^{\text{e}}$	< -7.75	-6.55	< -1.20

^aSolar photospheric abundances from Grevesse et al. (1996), except for O which is from Allende Prieto et al. (2001).

^b $[X/H] = \log (X/H) - \log (X/H)_{\odot}$.

^cAbundances in the northwest (NW) and southeast (SE) H II regions from Izotov et al. (1999) and Izotov & Thuan (1999). The same solar scale used for the neutral ISM has been adopted for consistency (column 5).

^dSum of the column densities of the two velocity components.

^eUpper limit is a 3σ estimate inferred from P II $\lambda 1152$.